Catalysis Communications 187 (2024) 106845

Contents lists available at ScienceDirect

Catalysis Communications

journal homepage: www.elsevier.com/locate/catcom

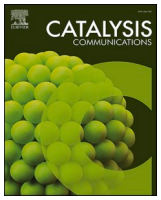

The roles of carbonaceous wastes for catalysis, energy, and environmental remediation

Chi Huey Ng [a,b,c,***], Mohd Aizzan Mistoh [a], Siow Hwa Teo [c,d,e,*], Andrea Galassi [g], Yun Hin Taufiq-Yap [e,f,**], Nancy Julius Siambun [a], Jurry Foo [h], Coswald Stephen Sipaut [a], Jeffrey Seay [i], Jidon Janaun [a,***]

[a] Faculty of Engineering, Universiti Malaysia Sabah, Jalan UMS, Kota Kinabalu 88400, Sabah, Malaysia
[b] Centre of Research in Energy and Advanced Materials, Faculty of Engineering, Universiti Malaysia Sabah, Jalan UMS, Kota Kinabalu 88400, Sabah, Malaysia
[c] Sonophotochemistry Research Group, Faculty of Science and Natural Resources, Universiti Malaysia Sabah, Kota Kinabalu 88400, Sabah, Malaysia
[d] Industrial Chemistry Programme, Faculty of Science and Natural Resources, Universiti Malaysia Sabah, Kota Kinabalu 88400, Sabah, Malaysia
[e] Catalysis Science and Technology Research Centre, Faculty of Science, Universiti Putra Malaysia, Serdang 43400, Selangor, Malaysia
[f] Institute of Plantation Studies, Universiti Putra Malaysia, UPM, Serdang 43400, Selangor, Malaysia
[g] Institute for Sustainability Science and Technology, Unversitat Polytècnica de Catalunya, Barcelona, Spain
[h] Faculty of Social Sciences and Humanities, Universiti Malaysia Sabah, Jalan UMS, Kota Kinabalu 88400, Sabah, Malaysia
[i] Faculty of Chemical Engineering University of Kentucky, 211 Crounse Hall, 4810 Alben Barkley Drive Paducah, KY 42002, United States of America

ARTICLE INFO

Keywords:
Carbon nanomaterials
Synthesis
Catalysis
Energy
Environmental remediation

ABSTRACT

This article reviews recent studies about various generations of the carbon materials for their applications in energy and environmental remediation. The synthesis routes of the carbon materials including the condition parameters, interaction of precursors, dopants and carbon materials, as well as their physical/chemical properties are explicated first. Then, the application and mechanism of metal-free/metal-doped/non-metal-doped carbon materials are discussed in detail. Lastly, this review is ended with a summary and invigorating perspectives on the challenges and future directions at the forefront of the catalysis platform to take a step further for real application.

1. Introduction

Carbon atom is viable in forming robust bonds in different modes with its four available valence electrons on its outer shell with many other elements. In addition, carbon is capable of forming carbon allotropes by sp., sp^2, and sp^3 hybridization configuration such as diamond, amorphous carbon, and graphite, which can be further modified to form graphene, carbon nanotubes, fullerenes, etc., consequently gave rise to structural, morphologies, and properties variations [1]. For instance, sp^2 hybridization makes the loose interlamellar coupling graphite layered structure, which can be exfoliated to form graphene [2]. Whereas, the hybridization of sp-sp^2 carbon atom leads to the formation of graphyne [3]. Research focus is also steering toward a more sustainable approach by using low specific energy input and biomass materials as the raw materials for potential applications in energy and environmental usage.

Falls in the group of the carbon family, chars derived from biomass or non-biomass compounds, have drawn considerable attention to date owing to their abundant and cost-effective properties. One of the significant disadvantages of biochar or char-based materials is their surface area. It should be noted that the surface area of biochar without pre/post-treatment is usually inferior to that of activated carbon (AC), making them unpersuasive for real practical application. For this reason, relentless efforts have been devoted to enhancing the surface area of biochar to a desirable extent by exploring different activation agents and methods. For example, the surface area of hardwood-derived biochar was substantially higher after being pre-treated with KOH at an ambient

* Correspondence to: Teo Siow Hwa, Industrial Chemistry Program, Faculty of Science and Natural Resources, Universiti Malaysia Sabah, Kota Kinabalu 88400, Sabah, Malaysia.
** Correspondence to: Taufiq-Yap Yun Hin, Catalysis Science and Technology Research Centre, Faculty of Science, Universiti Putra Malaysia, UPM, Serdang, Selangor, Malaysia.
*** Corresponding authors.
E-mail addresses: chihueyng@ums.edu.my (C.H. Ng), tony@ums.edu.my (S.H. Teo), taufiq@upm.edu.my (Y.H. Taufiq-Yap), jidon@ums.edu.my (J. Janaun).

https://doi.org/10.1016/j.catcom.2024.106845
Received 29 August 2023; Received in revised form 25 December 2023; Accepted 10 January 2024
Available online 11 January 2024

temperature [4]. Otherwise, hydrothermal treatment or oxygenation serves as an alternative approach that has shown significant contribution in increasing the surface area of rice straw-biochar at 700 °C in the presence of H_2O for 1 h [5]. Hydrothermal carbonization (HTC) yields carbonaceous materials of various sizes, shapes, and surface functional groups depends on the experimental conditions and reaction mechanism. Carbonaceous under high temperature HTC influence renders higher carbon content and exhibits graphitic structures. While lower temperature process gives rise to carbon material with surface functional groups, pore structures (micro or *meso*), and excellent reactivity, which is a potential in forming nanocomposites and hierarchical structures [6].

Graphene is an atom-thick sp^2 hybridized carbon with honeycomb-like structure, accompanied with large surface area of 2630 m^2/g, high thermal conductivity of ~5000 W/mK, abundant edges, and open channels that is viable for various energy and environmental remediation applications. Among the top-down and bottom-up graphene-based synthesis methods, chemical vapor deposition (CVD) is the most used method for graphene synthesis [7]. Graphene is hydrophobic and chemically inert, making it suitable for pollutant removal. On the other hand, graphene oxide (GO) is usually synthesized through graphite oxidation such as the Hummer's method. GO is composing of abundance oxygenated functional groups, depending on the types of precursor used (type of graphite or solutions) and the oxidation conditions. The hydroxyl and epoxy are lying on the basal plane, while the carboxyl and carbonyl are at the boundaries serve as active sites for certain chemical reaction [8]. Hence, GO could form stable suspension in solution and is readily used in various synthesis processes. But the number of these groups is highly dependent on the precursors used (type of graphite) and the oxidation conditions. Hence, GO could form stable suspension in solution and is readily used in various synthesis processes. When GO was underwent chemical or thermal reduction, partial functional groups would be eradicated and an excessive amount of defects would be formed, thus making it more chemically stable and excellent in electrical conductivity [9].

Apart from the biomass resources, waste materials such as plastics have great potential to be alternative feedstocks for carbonaceous production because plastic contains high carbon content. The transformation of plastic waste to carbonaceous can be executed through pyrolysis-carbonization, in which carbon can be molded into various dimensionalities and these carbon materials have been widely applied for energy and environmental applications. The discovery of CNTs have been widely applicable in the field of science and engineering owing to their unique physical and chemical properties including relatively high tensile strength, excellent chemical and environmental stability. CVD method is popular in commercially synthesizing CNTs in a fluidized bed reactor by channelling hydrocarbon vapor through a tubular reactor at 600–1200 °C in the presence of catalyst, ascribed to excellent growth rate, product yield, and development of the epitaxial thin film. CVD method is affordable for large-scale production; with an evident of scaled-up camphor CVD for MWCNT production has been commercialized in Japan [10]. The type of catalysts and their interaction, and the temperature are essential factors that affect the carbon yields. The common metals used in synthesizing CNT are Fe, Co, and Ni, which merits the carbon solubility at high temperature and enhance carbon diffusion. Moo and co-workers have successfully synthesized MWCNTs using plastic waste (LDPE, PP, and mixed plastics) as the feedstocks over a Ni-based catalyst via two-stage process (sequential pyrolysis and catalytic CVD) at two different temperatures of 500 °C and 800 °C. They clearly elucidated that CNTs synthesized at 500 °C was outperforming the one synthesized at 800 °C owing to CNTs at 500 °C possess higher density of edge defective sites (active sites) for ORR [11]. When Fe/Al_2O_3 composite catalysts were used in the CVD reaction, a well-aligned CNT arrays with lengths in a range of 500 μm to 1.5 mm were observed. Using Fe/Co/Al_2O_3 catalysts, on the other hand, revealed that the synthesis temperature has great influence on the CNT's diameter, quality and yield, which is yet to be clear [12].

Engineering metal-carbon hybrid materials for high catalytic activity is another option because the introductory of metal species into the carbon framework has proved to have promoted catalytic activity than the pristine carbon catalyst [13,14]. This phenomenon is credited to the stabilization of metals by the large surface area and pore size structure carbon material, consequently solves the existing metal aggregation and leaching issues [15,16]. Metals can be incorporated into the carbon material as nanoparticles or single-atomic metal, and both displaying their own advantages [17]. In addition, non-metallic heteroatoms such as S and N-elements are also added to the carbon materials to tune the electronic properties, as well as to provide localized grounds for metal chelation to enhance the catalytic ability of the metal-carbon hybrid materials [18]. Therefore, this review gives an overview of the synthesis of various sustainable carbononaceous from cost effective methods and resources, followed by the discussion of their applications in energy and environmental-related fields.

2. The emergence of carbonaceous catalysts

In compliance to the Sustainable Development Goal 7 (Affordable and clean energy, SDG 7), carbon-based catalysts have gained considerable attention within these recent years, either serving as catalysts or being supports in catalytic aromatization attributed to their high specific surface area, high porosity, excellent electron conductivity, relative chemical inertness, and flexibility of the products. Advantageously, carbon materials can be derived from coal and renewable biomass, thus promising for low cost and low carbon footprint. Carbon materials possess various oxygen functionalities, making them acid-base in nature and excellent carbon-supported catalysts [19]. These carbon materials can be activated under high-temperature conditions and chemically functionalized or decorated with metallic nanoparticles in strengthening their catalytic activity [19]. In this section, we will review the synthesis routes (Fig. 1) of the carbonaceous materials, including activated carbon (AC), biochars (BC), non-biochars, and zeolite-templated carbons (ZTCs), as well as their physical/chemical properties, morphological structures of each carbon nanomaterials.

2.1. Synthesis routes of the carbonaceous nanomaterials

Carbon materials fabricated from waste biomass have demonstrated promising applications as sorption materials, hydrogen storage, biochemical, biofuels, and so on. Nevertheless, the problem lies here: there is still no general and satisfactory process for producing valuable

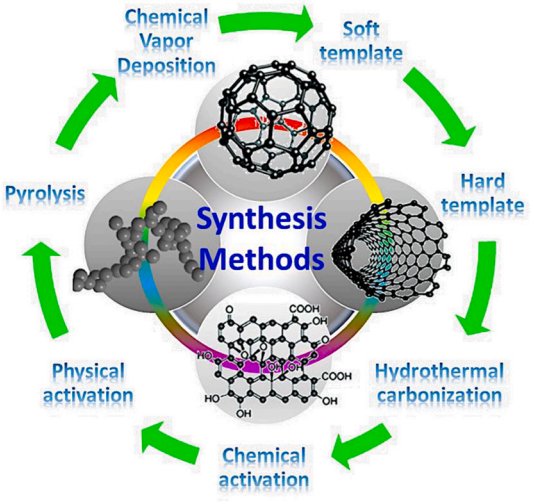

Fig. 1. The synthesis methods of carbonaceous materials.

carbon materials from crude biomass to date. Up to this date, hydrothermal carbon (HTC) materials have been of great interest to produce carbon materials with tunable physical and chemical properties for different applications ascribed to their low-cost, eco-friendliness, lightweight, and great potential for the energy and environmental research field. By combining the HTC with templating approaches, the HTC carbon structure can be highly improved in surface area and pore volume. Moreover, chemical and physical activations help to enhance the specific surface area and create porosity. An activation treatment process requires an additional treatment step with an activating agent at the initial carbon synthesis process before the carbonization process takes place, which helps in increasing the specific surface area and porosity of the carbon materials. In addition, the rich microstructures of natural biomass promote the formation of carbon materials with various dimensions, such as 1-Dimension, 2-Dimension, and 3-Dimension, through inheriting from various bio-template structures. In this section, we will look closer into the appealing strategies, which include activation methods, HTC methods, template approach, chemical vapor deposition, and carbonization methods that mold the carbon materials with satisfactory crystallinity, surface area, porosity, functional groups, active sites, and the unique properties associated with the dimensionality of carbon materials.

2.1.1. Hydrothermal carbonization (HTC)

HTC is a promising chemical route that converts organic solid wastes such as biomass, carbohydrates, organic molecules, and plastics into valuable carbon materials such as hydrochar, as well as for the synthesis of various new solids, functional oxide, and non-oxide nanomaterials with desirable shapes and sizes [20–22]. The carbon materials treated under hydrothermal conditions change solubility, melt crystalline parts, promotes physical and chemical interaction between reagents and solvent, facilitate ionic and acid/base reactions, and finally lead to the precipitation and formation of the carbonaceous structures. With the use of glucose, sucrose, starch, cellulose, algae, peanut shell, camphor leaves, bagasse, corn stover, coconut shell, and milk as the biomass precursors, porous carbon can be synthesized by the HTC process by heating biomass at a mild temperature in pure water and autogenous high pressure. Water in this reaction plays a vital role as a solvent to hydrolyze the glycosidic group in cellulose and hemicellulose of the biomass and catalyst to facilitate hydrolysis and cleavage of chemical structures of biomass for the production of porous hydrochar [23,24]. High ionization constant of water at high temperatures is responsible for the hydrolysis of organic compounds, which can further be catalyzed by acids generated during the reaction (e.g., acetic, levulinic, formic, or lactic). The presence of these organic acids accelerates hydrolysis and decomposition of oligomers and monomers to smaller fractions. The further hydrolysis leads to a complete disintegration of the physical structure of biomass. The difference in the chemical composition depends on the HTC reaction mechanism, which includes hydrolysis, dehydration, decarboxylation, aromatization, and re-condensation [25]. The first step of HTC reaction is hydrolysis which exhibits the lowest activation energy that breaks down the biomass chemical structure through cleavage of ester and ether bonds of bio-macromolecules with water molecules, giving rise to soluble (oligo-)saccharides and fragments of lignin that enter the liquid phase. The fragments of lignin are then hydrolyzed into phenols. Dehydration removes water from the biomass matrix that eliminates hydroxyl groups, while decarboxylation eliminates carboxyl groups in the process. The combination of dehydration and decarboxylation cause aromatization where double-bonded functional groups (e.g., C═O and C═C) replace the single-bonded hydroxyl and carboxyl groups in the biomass matrix [26].

The main controllable parameters of the HTC reaction mechanism are governed by the biomass feedstock, catalyst/additive, reaction temperature, and residence time. Jaroniec and co-workers summarized that the shape and surface properties of hydrochars are greatly dependent on the initial structure and composition of biomass precursors, attributed to a high degree of structural complexity and the differences in the solubility of intermediate products [27]. For example, monodispersed spherical hydrochars with diameters ranging from a hundred nanometers to a few micrometers, as shown in Fig. 2a-c, were derived from pure carbohydrate sources such as glucose and fructose, and starch. When the carbon feedstocks were changed to HTC of more complex biomass with different polymer chains such as cellulose, rye straw, and non-soluble carbohydrates in rice grains, morphological changes were inevitably observed for the formation of agglomerated/polydispersed spherical morphology or carbonized original fibrous biomass structure (Fig. 2d-f) [28,29]. In addition, the effects of additives and catalysts in controlling the structures and properties of carbon nanomaterials should not be marginalized. For example, whisker-like MnO_2/carbon sphere composites were synthesized by Wang et al. through a facile one-step HTC method using a mixed solution of glucose and manganese sulfate monohydrate [30]. The highly porous interconnected MnO_2 nanowhiskers-coated sphere exhibited a high specific surface area that favors the rapid transport of electrons and ions. Another work reported by Lamiel et al. has demonstrated that incorporating Ni, Co, and S elements on the carbon sphere influences the carbonization process, thus producing carbon materials with diverse structures and properties [31].

In addition, the reaction temperature is another factor that impacts the yield and porosity of the hydrochar. Depending on the experimental conditions and reaction mechanisms, HTC processes can proceed at either high temperature (300–800 °C) or low temperature (180–250 °C) [33]. A relatively low-temperature HTC process can generate monodispersed colloidal carbonaceous spheres from the carbohydrate sources such as sugar, glucose, fructose, sucrose, cellulose, and starch via dehydration and condensation polymerization and aromatization in the liquid phase [6]. Generally, at an elevated temperature, the hydrochar yield is considerably lower due to an intensified dehydration where immense volatile compounds are released from the biomass precursor at an elevated temperature condition, resulting in the formation of pores [34]. Optimizing the reaction temperature is essential to tune the structural property and morphology of the carbon materials. According to the discovery by Sun et al., they found that carbon spheres derived from glucose were only formable at 160 °C for 3.5 h with diameters of 200 nm, and the carbon spheres grew larger (1500 nm) by further increasing the temperature up to 180 °C for 10 h. Furthermore, a longer time is needed to hydrolyze the HTC of polysaccharides and biomass into smaller pieces. For instance, it takes 10 h for the transformation of monosaccharide glucose into uniform carbon nanospheres at 180 °C (Fig. 2g), but c-furfural needs an even longer reaction time (24 h) for the formation of carbon spheres with different diameters (Fig. 2h) [32,35]. While, when the temperature of the HTC process exceeds 300 °C, reactive gases and carbon fragments produced from thermolysis are apt to synthesize various dimensional carbon nanomaterials such as the carbon nanotubes, graphite, and activated carbon materials [6]. These unique morphologies of dimensional carbon nanostructures are not merely excellent bio-templates to fulfill excellent electrochemical properties but also the building blocks for flexible electrodes.

Until now, plenty of parameters, including precursors type, reaction temperature, duration, and additives, have been recorded for the development of carbon nanomaterials, as mentioned in the earlier section. However, one may naturally question whether this current HTC process is sufficiently applicable for synthesizing carbon nanostructures with controllable morphological structure and physical properties such as attaining desirable porosity and specific surface area? To secure the desirable properties of the carbon nanostructures, several extending approaches, such as templating and activation methods, were tandemly performed together with HTC to generate pore ordering in carbons.

2.1.2. Template approaches

Templated carbonization is an appealing method for synthesizing three-dimensional porous carbon at the nanoscale, where pore sizes range from 1 to 200 nm and even an ordered pore structure [36].

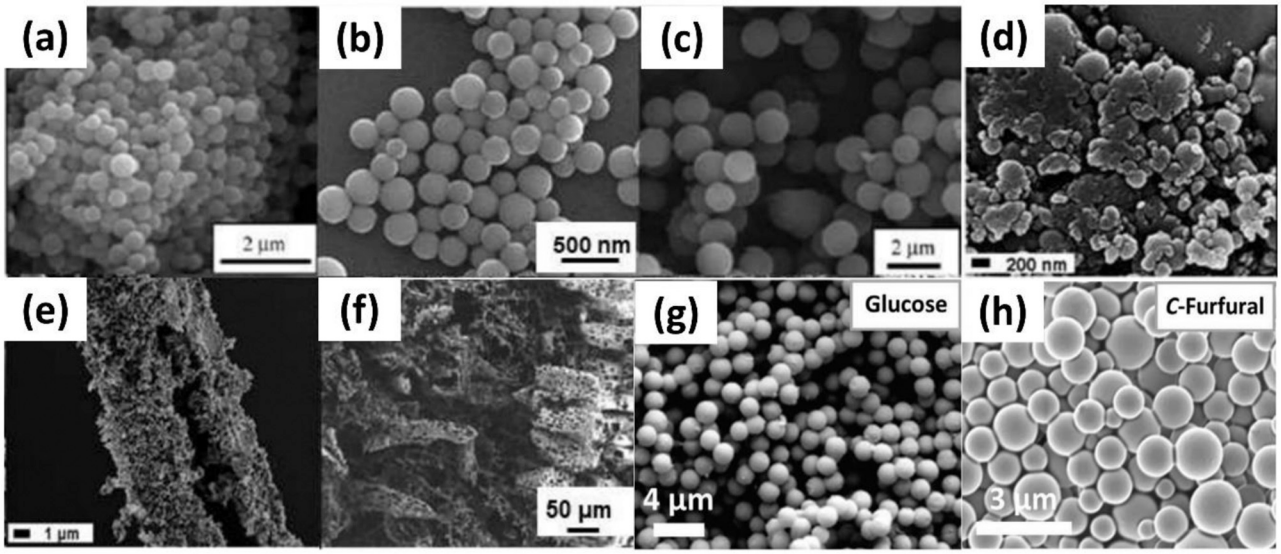

Fig. 2. SEM images of hydrochar produced from (a) glucose, (b) sucrose, (c) starch, (d) cellulose, (e) rye straw, and (f) the non-soluble carbohydrates in rice grains. Reproduced with permission [27]. Copyright 2020, Royal Society of Chemistry. Hydrothermal carbonization of different biomass. (g) SEM image of carbon spheres prepared from glucose (180 C, 10 h) and (h) SEM image of carbon spheres prepared from c-furfural (180 C, 24 h). Reproduced with permission [32]. Copyright 2021, Wiley-VCH.

Researchers have exhaustively explored the controllable nanostructure design of biomass-derived carbon, such as porous, hollow, etc., has been exhaustively explored by researchers through the hard and soft template synthesis process [37]. The carbon materials' porosity, morphology, and surface area are easily tuned by appropriate templates, making them (carbon catalysts) applicable in various applications. Templated

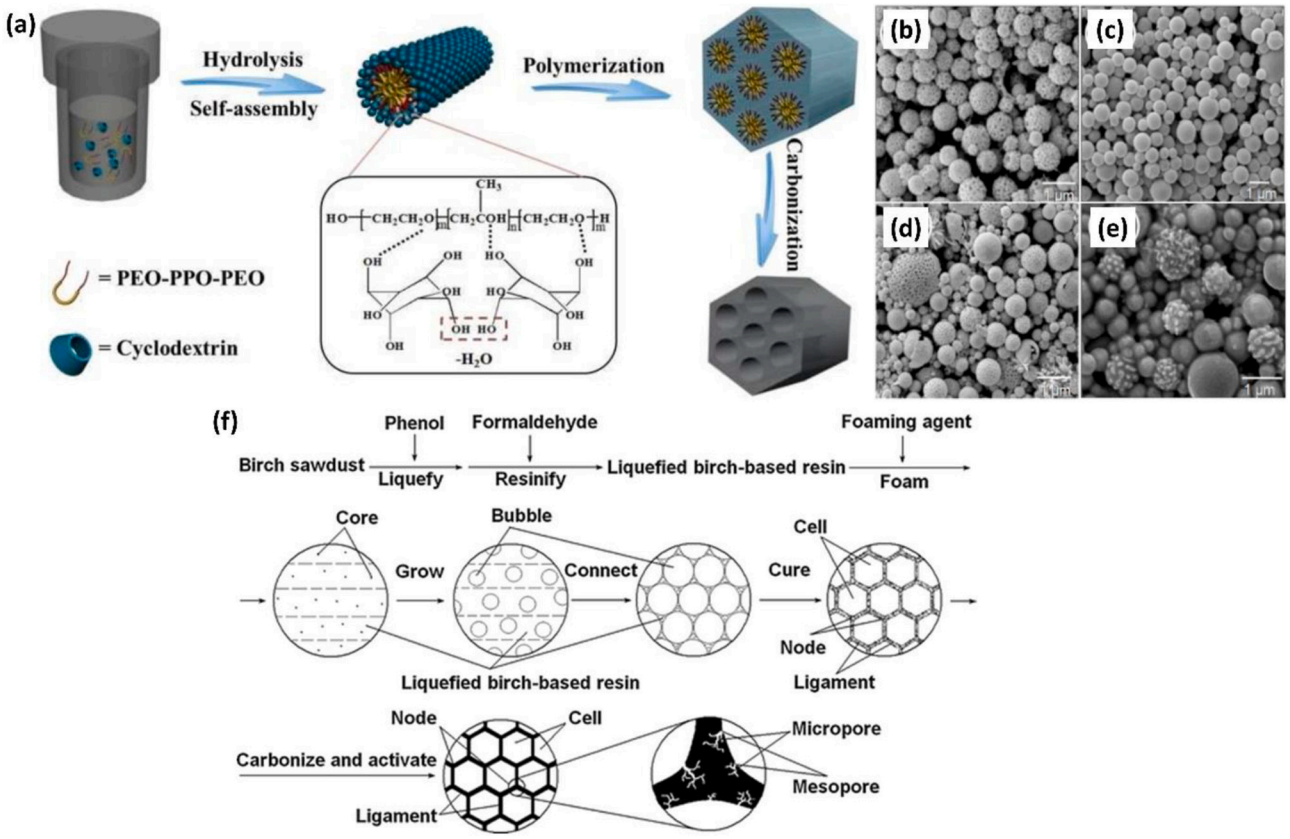

Fig. 3. (a) A synthetic illustration of the ordered mesoporous carbon material derived from β-cyclodextrin precursor through successive hydrothermal treatment (at 140 °C) and carbonization treatment (at 700 °C). Reproduced with permission [39]. Copyright 2014, Royal Society of Chemistry. SEM images of (b) CS-L prepared from liquefied larch, (c) CS-R prepared from liquefied larch resins, (d) CS-L-F prepared from liquefied larch and F127, (e) CS-R-F prepared from liquefied larch resins and F127. Reproduced with permission [41]. Copyright 2018, Elsevier. (f) Formation mechanism of carbon foams. Reproduced with permission [42]. Copyright 2011, Springer.

carbonization is divided into soft template and hard template strategies [38].

The soft template is usually formed by organic molecules such as non-ionic surfactants and ionic micelles, developing a framework when contacting a given material. The relatively "greener" soft template process alters various morphologies of carbon materials and simplifies carbon formation's synthesis route. Soft templating guarantees the construction of carbon materials of controllable micro-, meso-, or macro-structures. Nevertheless, it is less favorable for the synthesis of biomass-derived carbon materials due to the low thermal stability of organic molecules. In most cases, hydrothermal carbonization or other processes are always complemented to stabilize the formed structures by templates and carbon precursors. For instance, Zhao and co-workers have successfully synthesized highly ordered mesoporous carbons (OMCs) via hydrothermal process. They used β-cyclodextrin (β-CD) as the biomass carbon precursor and triblock poly(ethylene oxide)-poly(propylene oxide)-poly(ethylene oxide) (PEO-PPO-PEO) copolymer as the soft template (Fig. 3a) [39,40]. β-CD was chosen as the carbon source, attributed to its cyclic oligosaccharides consisting of a porous-shape structure with a hydrophobic cavity and hydrophilic rims made of hydroxyl groups. The resultant mesoporous carbons displayed a highly ordered mesostructured with a 2D hexagonal *p6mm* symmetry, a high specific surface area of 781 m^2/g, and a large pore size of ~4.5 nm. Another typical example of soft-templating carbon nanostructured is the mesoporous featuring carbon with spherical morphology. These carbon spheres were developed by Zhao et al. by utilizing an ultrasonic spray pyrolysis technique using F127 as a sacrificial template [41]. In the earlier reports, mesoporous carbon spheres were synthesized through nanocasting technology coupled with the hydrothermal method but were unfavorable due to longer time and higher cost expenses, accompanied by tedious and complicated procedures. Thus, ultrasonic spray pyrolysis technology is taking the role of spherical carbon development. Based on the discovery by Zhao et al., alteration of morphology and porous structure of the carbon spheres were obvious by controlling the used precursors and F127 [41]. Carbon spheres are derived from liquefied larch (CS-L) and liquefied larch-based resins (CS-R) either with or without F127 templates. The carbon spheres with templates are therefore denoted as CS-L-F and CS-R-F. SEM images show that the surface morphology of carbon spheres changed when different carbon precursors were used. The morphological structure of carbon spheres derived from larch, either in its pristine form or template, is similar; they possess uniform honeycomb-like spheres with a size of 600–900 nm (Fig. 3b and d). Whereas, when larch-based resins were used to develop the carbon spheres, it is expected that the prepared foams consist of adjacent cells, ligaments, and nodes arranged in an irregular pentagon or hexagon in a cell size of 100–200 μm (Fig. 3f). The increasing carbonization temperature shrinks the cell and makes it more uniform. Consequently, it gave smoother carbon spheres, as displayed in Fig. 3c [42]. Nevertheless, templating CS-R with F127 further changed the morphological structure of CS-R-F to a walnut-like shape. The change of surface structure could be ascribed to the decomposition of F127 with resins (Fig. 3e) that have created abundant pores. Overall, despite soft-templating simplifying the production of porous carbon without the need for template removal, self-assembly between biomass derivatives and micelles is indeed weak. The carbon materials derived from the soft-template method are incompatible for the high-temperature pyrolysis process due to surfactant molecules' inherent instability. In addition, the soft templates are usually expensive polymers and non-renewable, thus restraining their wide applications. In most cases, soft templated carbon nanomaterials are desirable in electrochemical energy technologies, particularly for the development of electrodes [43].

Apart from the soft-template synthesis of biomass-derived carbon, the hard-template method is regarded as a promising nanocasting approach for the development of nanostructured carbon, which usually involves several key processing steps, including (1) synthesis of desired hard templates, (2) impregnating the as-prepared templates with solute biomass precursors, (3) high-temperature treatment or template composites in an inert atmosphere, and (4) removal of hard templates using acid or alkaline solvents. In this approach, hard templates are employed to design various geometries and structures of carbons with length scales of nanometers and micrometers and the construction of hierarchical pore architectures. The typical sacrificial templates applied for the construction of carbon nanohybrids are thermally stable, such as microporous zeolite, mesoporous silica, nano SiO_2, $CaCO_3$, MnO, and MgO, which are easily prepared and commercially available, and are not deformable during carbonization. [36,44,45] Compared to soft-templating, tuning the structures and architectures of carbon materials through hard-templating is comparatively more straightforward and common. In 2019, Luo et al. designed a unique hierarchical porous carbon microcubes, denoted as PCM, via an in-built template method from renewable agaric (Fig. 4a) [46]. The cubic MnO@C composite was obtained by hydrothermal treatment of agaric, followed by calcination in the presence of a manganese (Mn) source. The in-built MnO template is sacrificed by acid etching, giving rise to PCM formation with a high specific surface area of 1052 m^2/g, rational pore size distribution, and self-N-doped properties. On most occasions, SiO_2 spheres are used as hard templates for constructing hollow spheres and porous carbon. For example, a 3D N-doped porous carbon (NPC) was prepared via a simple SiO_2 nanosphere-assisted pyrolysis method. [32] Liu and co-workers prepared N-doped carbon nanodots through hydrothermal carbonization using shrimp shells as the carbon and nitrogen sources. SEM and TEM images display that the 3D NPC exhibits uniform pores (200 nm) (Fig. 4b and c), indicating increased active sites for diverse applications. In addition, ordered mesoporous silica templates such as SBA-15, SBA-16, KCC-1, and KIT-6 have been served as hard templates for highly ordered porous carbon nanostructures. The ordered mesoporous structure plays a vital role in high specific surface area and pore volume. In the case of Qu et al., biomass waste (gelatin) was used as the precursor, and SBA-15 serves as the hard template for preparing nitrogen-doped ordered mesoporous carbon (NOMC). An appropriate nitrogen doping, high pore volume, and desirable specific surface area of NOMC are prominent for the catalytic reaction [47]. Another example, KIT-6, was used by Bai et al. as the hard template for synthesizing ordered mesoporous carbon using biowaste lignosulphonate, as shown in Fig. 4d [48]. Typically, sodium lignosulphonate was impregnated into the KIT-6 template, and the resultant product was carbonized. The silica template was removed using NaOH solution to obtain ordered mesoporous carbon (OMC). Then, the ordered carbon was chemically activated using $ZnCl_2$ for hierarchical ordered porous carbon (HOPC). It was hypothesized that the lignosulphonate molecules were adsorbed onto the hydrophilic silica walls through hydroxyl groups and cross-linked through hydrogen bonds, forming 3D networks that increase the pore volume, as well as bridge the aromatic rings to promote graphitization. It is anticipated that hard template-assisted methods effectively construct porous carbon structures for emerging applications in catalysis and the fields of batteries and supercapacitors.

On the whole, the exploration of novel templates and environmentally friendly chemical etchants for the family of hard- and soft-template carbon nanostructured is underway and is gaining momentum among all research scientists at present for the breakthroughs and advances in this emerging frontier of science and technology. It is genuinely believed that the diverse types of hard- and soft-template biomass-derived carbon-based nanostructures will continue to proliferate to develop a myriad of catalytic systems for thermochemical conversion reactions and other catalytic reactions for a sustainable future.

2.1.3. Activation approaches

Carbonaceous nanomaterials derived from renewable biomass have been at the forefront of nanotechnology research owing to their abundant availability, cheaper raw materials, reusability, non-toxic nature, and biodegradability. Carbon material synthesized from biomass is efficient support for active sites due to its high porosity and surface area

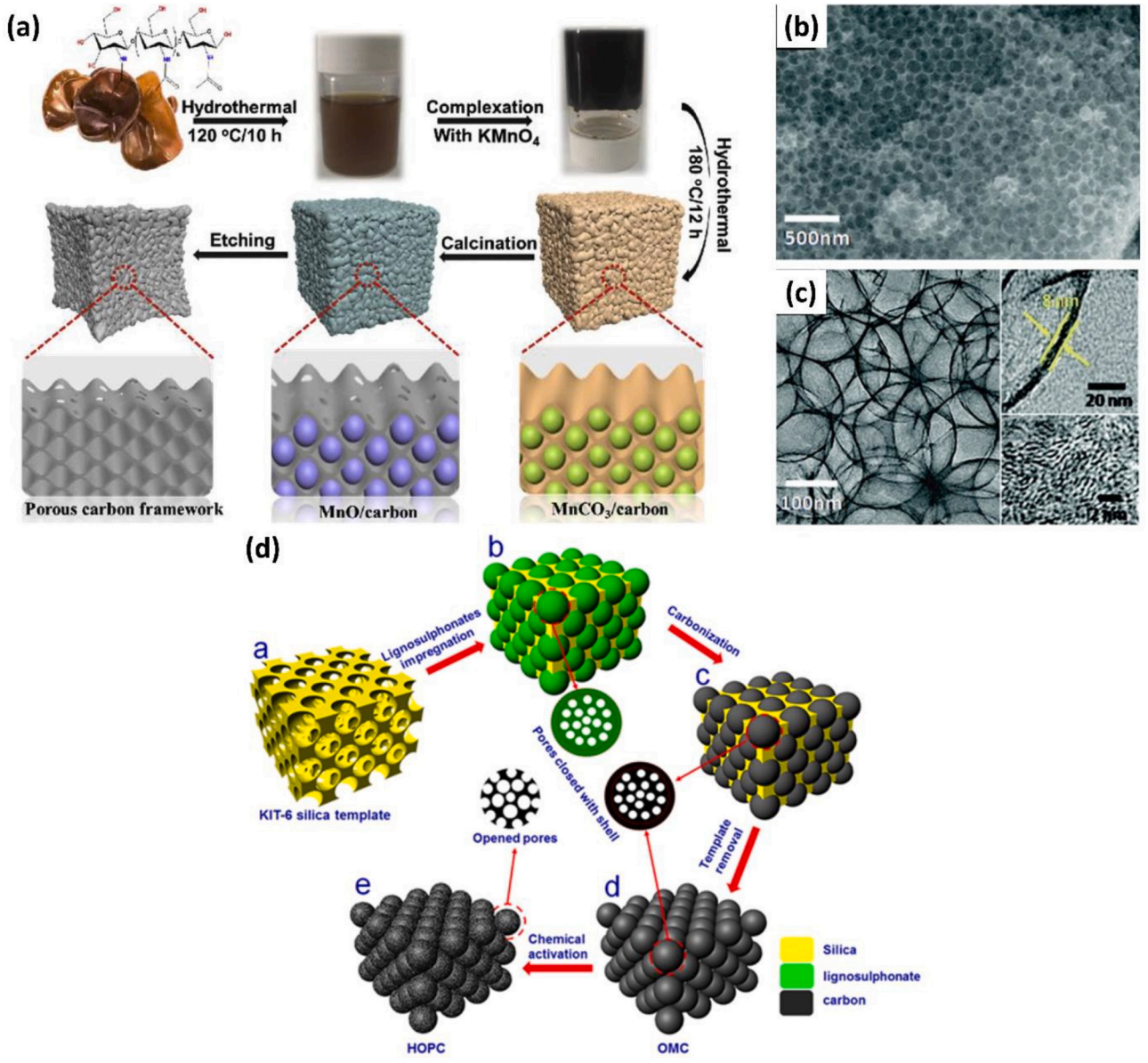

Fig. 4. (a) Schematic illustration of the preparation and morphology of the PCM sample. Reproduced with permission [46]. Copyright 2019, Elsevier. (b) SEM image of the NPC obtained at 800 °C, (c) TEM image of the NPC obtained at 800 °C and the corresponding TEM images of NPC pore wall. Reproduced with permission [32]. Copyright 2021, Wiley-VCH. (d) illustration of the synthetic processes of hierarchical ordered porous carbon (HOPC) using the hard template method combined with post chemical activation. Reproduced with permission [48]. Copyright 2020, Springer.

characteristics, and these traits are highly tunable depending on its pre-treatment methods. An additional treatment step using an activating agent is essential before the carbon synthesis process because the internal porous structure of the carbon material would develop at this particular step for the inherent of high mass transfer capacities and high active loading surface for catalysis purposes [49]. For this reason, strenuous efforts have been devoted to exploring novel activation methods, either in the forms of physical or chemical activation, to prepare porous carbon nanomaterials with unique morphologies. The former process is meant to physically activate carbon materials under a controlled flow of steam or CO_2 or a mixture of both at temperatures higher than 700 °C. It is inferred that activating gases would selectively uproot the reactive carbon components of the carbonized material via the C-H_2O and C-CO_2 gasification reactions after that unfolded the enclosed pores and interpenetrated with other pores [50]. It is widely reported that the types of activating gases, biomass type, and reaction conditions are crucial factors that influence the carbon materials' physicochemical properties, such as specific surface area, porosity, and pore size distribution. For example, char-derived from palm petiole was activated under CO_2 flow at various temperatures of 750 °C, 850 °C, and 950 °C for 30 min [51]. The palm petiole-derived char exhibited the highest specific surface area when the activation temperature was increased to 850 °C. With the increasing activation temperature, the total pore volume of the char plunged owing to the decomposition of material at high temperature under an oxidizing atmosphere, which implies the importance of optimizing the activation temperatures for the sake of carbon's physical properties [51]. In another work by Nguyen and co-workers, the authors emphasize the effect of physical activation using CO_2 and steam agents on the physicochemical properties of AC produced from a fern species named *Dicranopteris linearis* (*D. linearis*) [52]. The *D. linearis*-derived chars were made under pyrolysis at 400 °C for 1 h and were activated in various CO_2-steam proportions. Reflected from the IR and Raman spectra, the structure of the activated chars was heavily dependent on the relative ratio of CO_2 and steam, in which the

chars activated under CO_2^- and steam saturated conditions possess greater specific surface area than the pristine char. Moreover, as a result of the reaction between CO_2/steam and char, the highly porous activated chars are encompassed with micro-and mesopores structures owing to the diffusion of steam (smaller size water molecules than CO_2 molecules) within the carbon matrix that has efficiently catalyzed the char matrix, after that predominantly creating mesopores. These findings are indeed helpful in designing the AC with unique properties by simply tuning the proportion of steam and CO_2 [52]. Nevertheless, a contradiction arose when Nabais et al. demonstrated that the CO_2-activated biochars from coffee endocarp exhibited higher surface areas and pore volumes than the corresponding steam-activated biochars. This contradiction could be the implication of using different microstructures of biomass, which is related to the issue of feedstock types [53].

While, for the case of chemical activation, carbon-derived from biomass is first impregnated in a solution containing activating agents such as KOH, $ZnCl_2$, K_2CO_3, H_2SO_4, H_3PO_4, etc. for the promotion of pores formation through the removal of partial carbon atoms from the carbon matrix, suppress the formation of tar, and facilitate the evolution of volatile compounds, followed by heating at elevated temperatures under an inert gas flow [50,54]. Comparing against the physical activation, the chemical activation mechanism is still unclear. However, it is assuring that chemical activation possesses higher activation efficiency than the physical for the shaping of bio-carbon with higher surface area and porosity, even at relatively lower temperatures. Similar to the physical activation approach, the activation temperature, types, and doses of activating agents and feedstocks are the variables controlling the porosity, pore size distribution, and the specific surface area of the biomass-derived carbon. In the work of Dehkhoda et al., they highlighted the importance of optimizing the activation temperature toward the influence on the surface area and porosity of the biochar [55]. They showed that a substantial increment in surface area of biochar was observed from 1.66 m^2/g to 614–990 m^2/g when biochar was impregnated in KOH solution at an optimized activation temperature. However, the unfolding of pores in the biochar matrix devastated at increased activation temperature due to the collapse and burn-off of micropore walls and the development of localized graphite-like structure in the biochar matrix, thus reducing the desired surface area of the biochar [55]. In addition, the choice of activating agents is another factor that could adjust the properties of the carbon materials. Difference activating agents were used by Park and co-workers such as HCl, H_2SO_4, H_3PO_4, KOH, MgO, $ZnCl_2$, and K_2SO_4 to chemically activate the sesame straw biochar for the application in phosphorus adsorption. They discovered that ZnCl and MgO were more effective for phosphorus adsorption than the other activating agents [56]. Depending on the type of carbon materials, the properties of the carbon materials are altered upon activation. Harmas et al. showed that the carbon derived from glucose using KOH and $ZnCl_2$ exhibited a similar specific surface area at 2150 m^2/g. When rubber seed pericarp was used as carbon feedstock to replace the glucose-derived carbon material, the specific surface area of $ZnCl_2$ activated carbon exhibited a higher specific surface area (1689 m^2/g) than that of KOH activated carbon (392 m^2/g) [38,57]. In summary, it is crucial for us to carefully consider the factors, including types of feedstocks and pre-treatment parameters for desirable specific surface area and porosity of the formed biochar.

2.1.4. Chemical vapor deposition (CVD)

CVD is a powerful technique of depositing one or more volatile vapor reactants such as ethylene and acetylene into solid phase deposit upon the occurrence of chemical reaction [58]. This method is probable in producing zeolite-templated carbons (ZTCs), which is an ordered microporous carbon with zeolite as the sacrificial scaffold. As opposed to the ordered mesoporous carbons obtained from using mesoporous silica templates, it has been described that ZTCs comprise the curved and single-layer graphene frameworks accord for uniform micropore size of ca. 12 nm, high surface area of 4000 m^2/g, good compatibility with chemical modification, and coupled with elasticity [59]. Unlike the classical activated carbon features with highly disordered cross-linked structure, randomly packed graphene subunits connected through amorphous carbon components, ZTCs feature textural and morphological characteristic of the zeolite scaffolds. Among the variant zeolite frameworks, FAU, EMT, and BEA zeolite structures are the suitable templates, ascribed to their large voids (>0.6 nm) and 3D interconnected micropore systems [60]. Aumond and co-authors elucidate that small particle size of microporous materials offers higher effectiveness factors in a specific catalytic process owing to the implication of shorter diffusion path length. The authors disclosed that larger crystal size (3 μm) of Y zeolite templates resulted in portion of unfilled pores in the crystals' center. Moreover, employing a medium-sized beta zeolite (0.5 μm) template resulted in higher structural ordering than the larger (1 μm) crystals [60].

Basically, the penetration of carbon into the nanochannels of zeolites by CVD method happens in three steps, taking into account of the reaction temperature and reaction duration:

(i) Diffusion of carbon from the exterior (surface) of zeolite particle to the interior channel
(ii) Constant increasing rate of carbon density
(iii) Termination of carbon deposition

The key point for a CVD method is the reaction temperature because each CVD source gas possesses its thermal decomposition temperature where beyond the threshold limit, the gas turns into soot even without the presence of catalyst. Taking an example of acetylene and propylene with decomposition temperatures of ca. 923 K and 1023 K, respectively, the exterior of the zeolite particles will be deposited with carbon (forming a Type-II ZTCs consisting non-templated carbon deposition) if the decomposition temperature of gases have been exceeded. Hence, the CVD temperature should be lower than the decomposition temperature for obtaining a 3D ordered ZTC framework replicated by the zeolite template [59]. Moreover, Nishihara and co-workers have also disclosed that a two-step CVD operates at different temperatures offer Type-I ZTCs with high surface areas up to 3370 m^2/g [59,61]. Another key feature of controlling temperature is that high temperature demerits reaction selectivity that leads to structural defects and random morphological orientation, despite high temperature promotes mass transfer and improves heteroatoms doping possibility. Mokaya et al. synthesized N-doped CNTs using NH_4-zeolite β as the template, ferric nitrate as the catalyst, and acetonitrile as the carbon source. The CVD reaction was performed at various temperatures from 700 to 900 °C for 20 h (Figs. 5a-h). The length of the aligned CNTs elongates with the increasing temperature and aligns better with sufficient growing duration (longer reaction duration), as shown in Figs. 5i-k, but is distorted (randomly oriented and broken nanotubes) at 900 °C. The work of Nishihara et al. displayed that carbon deposited rapidly into the zeolite voids at the first 0.5 h (stage 1), followed by a decelerating deposition rate from 0.5 to 5.8 h (stage II) due to narrower pores of zeolite (Fig. 5l). From the TEM images, it is apparent that crack-like space appeared in the zeolite particle at the second hour and gradually disappearing as time passed. After reacting for 8 h, carbon is uniformly distributed and deposited in the zeolite pores, as shown in Figs. 5m-p. In brief, CVD merits the growth of nanocarbon in terms of its alignment, density, and diameter of the nanocarbon per se, in addition to favouring large scale production.

2.1.5. Carbonization

Anoxic pyrolysis carbonization is a high temperature process to transform plastic waste into carbon-based materials in a tube furnace. The carbonization temperature plays an integral role for the tuning of product's physicochemical properties where high carbonization temperature above 700 °C guarantees for porosity and conductivity with less contain of oxygenated groups [62]. Subsequently, post-activation either through physical or chemical approaches should be employed to tailor

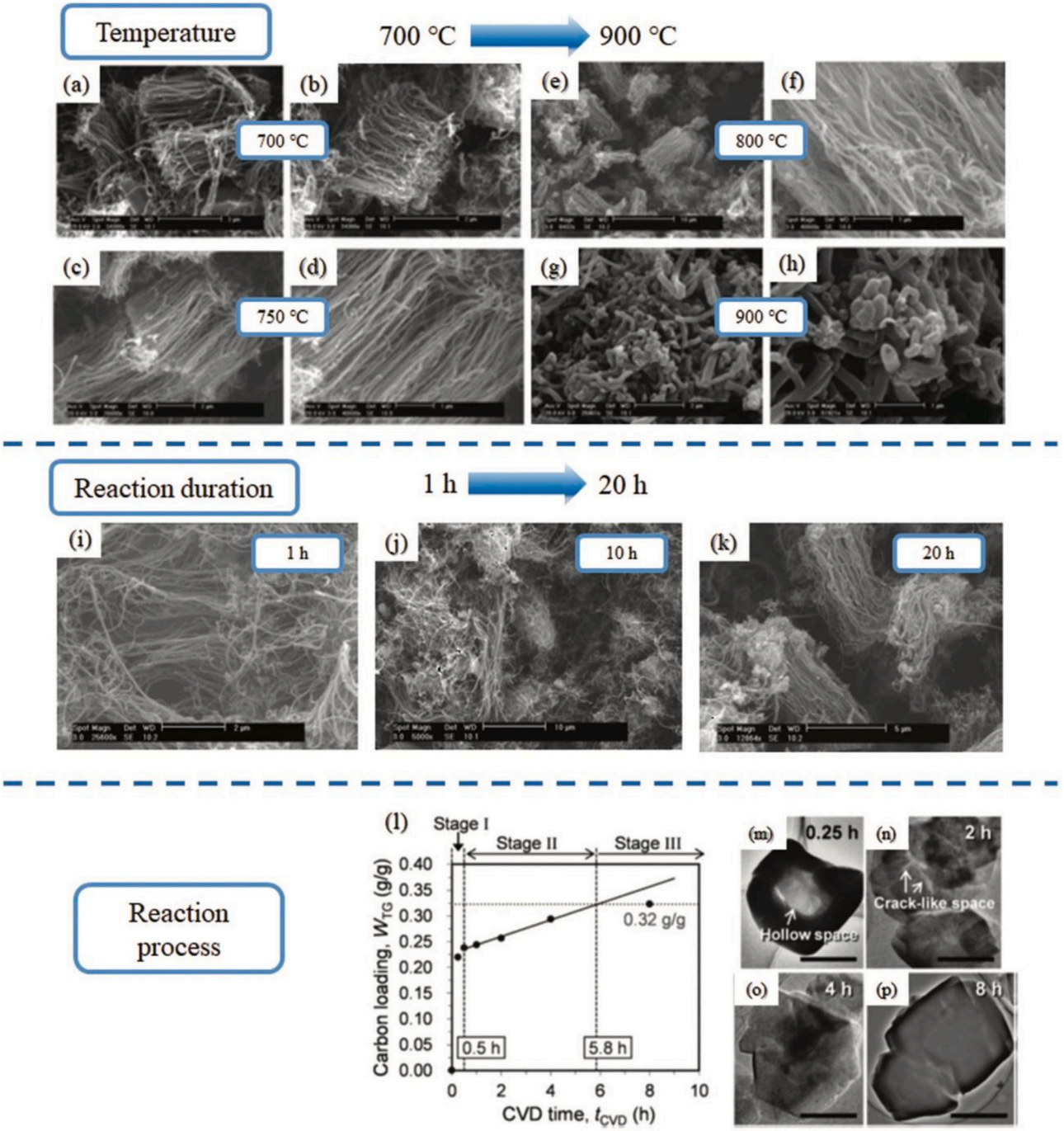

Fig. 5. (a)-(h) Influence of temperature and reaction duration on synthesis of zeolite-templated nanocarbons: SEM images of CNTs, using NH_4-zeolite β as template and acetonitrile as carbon source, prepared at various CVD temperatures: a,b) 700 °C; c,d) 750 °C, e,f) 800 °C; g,h) 900 °C. i-k) SEM images of carbon nanotubes prepared via CVD at 800 °C using NH_4-zeolite β as substrate and acetonitrile as carbon source for various CVD durations: i) 1 h; j) 10 h; k) 20 h; l) the relation between WTG and t_{CVD}. m-p) Corresponding TEM images of liberated carbons in the particles of zeolite at t_{CVD} of 0.25, 2, 4, and 8 h. Scale bars are 1 μm. Reproduced with permission [2]. Copyright 2020, Wiley.

the properties of plastic derived carbonaceous (discussed in section 2.1.3). Evidently, a KOH-activated tyre pyrolysis char displayed excellent adsorption ability toward bisphenol A than a commercial activated carbon, thanks to the formation of large specific surface area of 700 m^2/g and high porosity upon activation [63].

On the other hand, catalytic carbonization is a mature technique for transforming plastic waste into carbonaceous materials such as CNTs, carbon nanosheets (CNS), graphene, and hierarchically porous carbon (HPC) with the assistance of catalysts. Catalyst in this case undergoes structure reconstruction during catalytic carbonization where the catalyst promotes the initial decomposition of plastic into liquid and gaseous products and the decomposed material serves as the feedstock to form the carbon material on the catalyst surface [64]. Series of catalysts such as organically modified clay (OMC)/nickel catalysts, zeolite/NiO, chlorinated compound/Ni_2O_3, activated carbon/Ni_2O_3, and carbon black/Ni_2O_3 were used to convert PP to produce aromatic compounds, which is subsequently dehydrogenated and reassembled into CNTs [65]. Using Ni, Fe, and Fe—Ni as the catalysts for catalytic carbonization of PP, PP was first pyrolyzed to hydrocarbons where the carbon and hydrogen precursors were further for catalytic decomposition process.

The bimetallic Fe—Ni catalyst was outperformed the monometallic Ni and Fe catalysts, attributed to the rapid diffusion of carbon intermediates on the surface of catalyst, leading to the formation of MWCNTs (Fig. 6) [62]. The summary of advantages and disadvantages of each synthesis route is tabulated in Table 1.

Table 1
Advantages and disadvantages of carbon synthesis methods.

Method	Advantages	Disadvantages
Hydrothermal carbonization	• Relatively low operating • Easy control of condition parameters	• Require sample separation steps and drying of the sample for further use
Chemical activation	• High yield production • Lower in cost • Simple recovery of the activating agents	• Requires through washing step
Pyrolysis carbonization	• Controllable carbonization temperature • Controllable heating rate	• High energy consumption • Require of high temperature operation
Soft templating	• Controllable pore structures and pore size	• Easy collapse of porous framework • Require template removal
Hard templating	• Develop nanostructured carbon • Efficient in constructing hierarchical pore architecture	• Removal of template using acid/alkaline • Require high temperature treatment
Chemical vapor deposition	• High deposition rate • High productivity	• Lack of high volatile and non-toxic precursors

3. Applications of carbonaceous nanomaterials for energy and environmental remediation

The emerging carbonaceous materials as promising electrocatalysts for various energy and environmental applications in the field of energy storage, conversion, CO_2 reduction, hydrogen production, heavy metals removal etc. have caught considerable interest, credited to their excellent conductivity, high surface area, and low cost. The pristine carbonaceous (without any modifications) is actually non-reactive due to electroneutrality of carbon atoms [66]. Hence, various approaches such as introducing doping heteroatoms into the carbon skeleton and assembling carbon atoms into different dimensions and structures (zero-dimensional (0D), one-dimensional (1D), two-dimensional (2D), and three-dimensional (3D)) have been strategies to design carbonaceous catalysts with remarkable activity. Fig. 7 shows the classification of various dimensionalities' carbon allotropes. According to the relevant reaction mechanisms, different carbon allotropes exhibit various bonding capacities with the reaction intermediates, leading to the formation of diverse products [66].

3.1. Energy

3.1.1. First-generation carbon materials

Renewable biomass such as bamboo, walnut shell, corn husk, etc. (Fig. 8) is an attractive activated carbon precursor that have been studied extensively for the development of sustainable products. These biomasses has a natural fine structure composed of mainly lignin (27%), cellulose (43%), and hemicellulose (20%) that have high carbon content and low ash content of 0.2–10%. These biomasses retain the natural AC's structure that contribute to the circulation of electrolytes and improve the performance on the electrochemical level [67]. Activated carbons from these biomasses have been extensively used as electrode material for supercapacitors, ascribed to its high surface area, tunable pore size and distribution that merits the energy storage via electric double layer (EDL). However, the supercapacitor electrode derived from corn-husk suffers from poor capacitance and retention <2000 cycles of charge-discharge owing to this material turns resistive after 2000 cycles [68]. This phenomenon could be ascribed to low conductivity caused by an undesirable porosity and surface area that can be overcome by opting an appropriate carbon precursor and activation mode in the synthesis route. Using corn-husk as the carbon precursor, the capacitive performance of the AC supercapacitors activated by KOH is different from the K_2CO_3 where the latter (K_2CO_3 activation) exhibited remarkable capacitive retention of ~99.5% of its original capacitance after 20,000 charge-discharge cycles, as compared to 90% capacitance retention (KOH activation) after 5000 cycles [68]. Non-metallic heteroatom doping such as N, B, O, P and S fine tunes the charge storage capability and surface chemistry of carbon matrix, and contributing to pseudo-

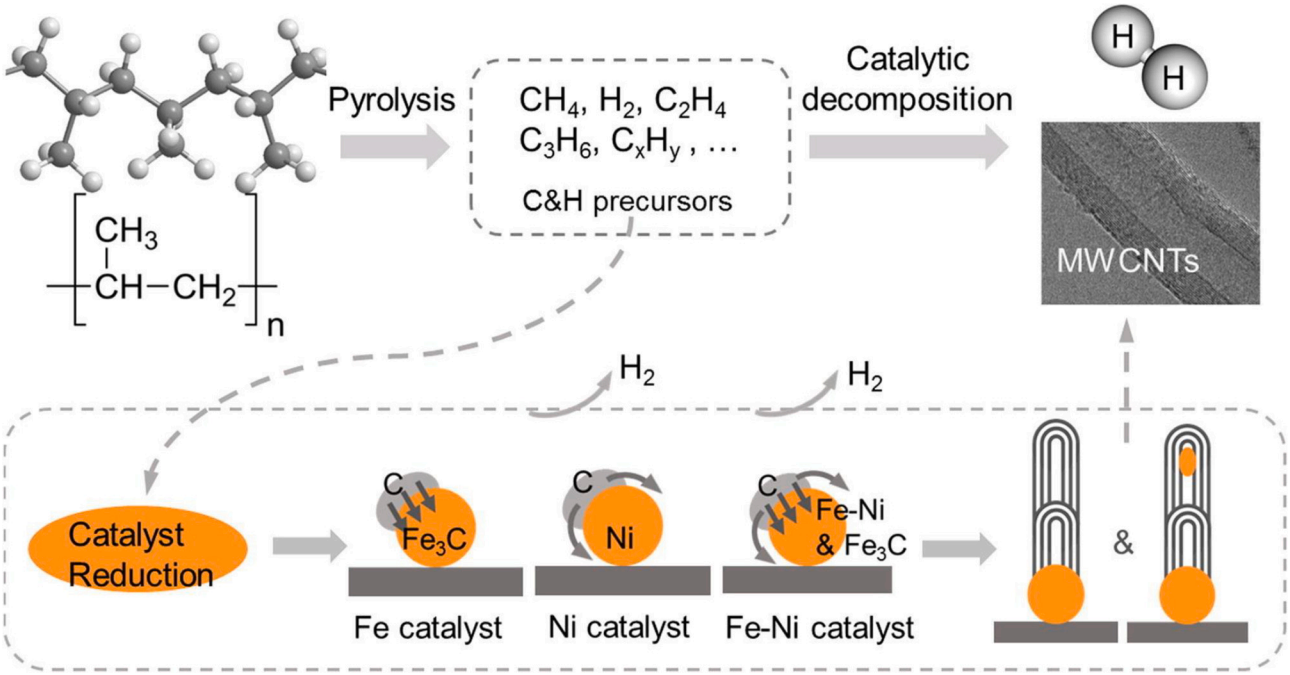

Fig. 6. Diagram of the catalytic carbonization of polypropylene with an Fe/Ni catalyst. Reproduced with permission [62]. Copyright 2020, Elsevier.

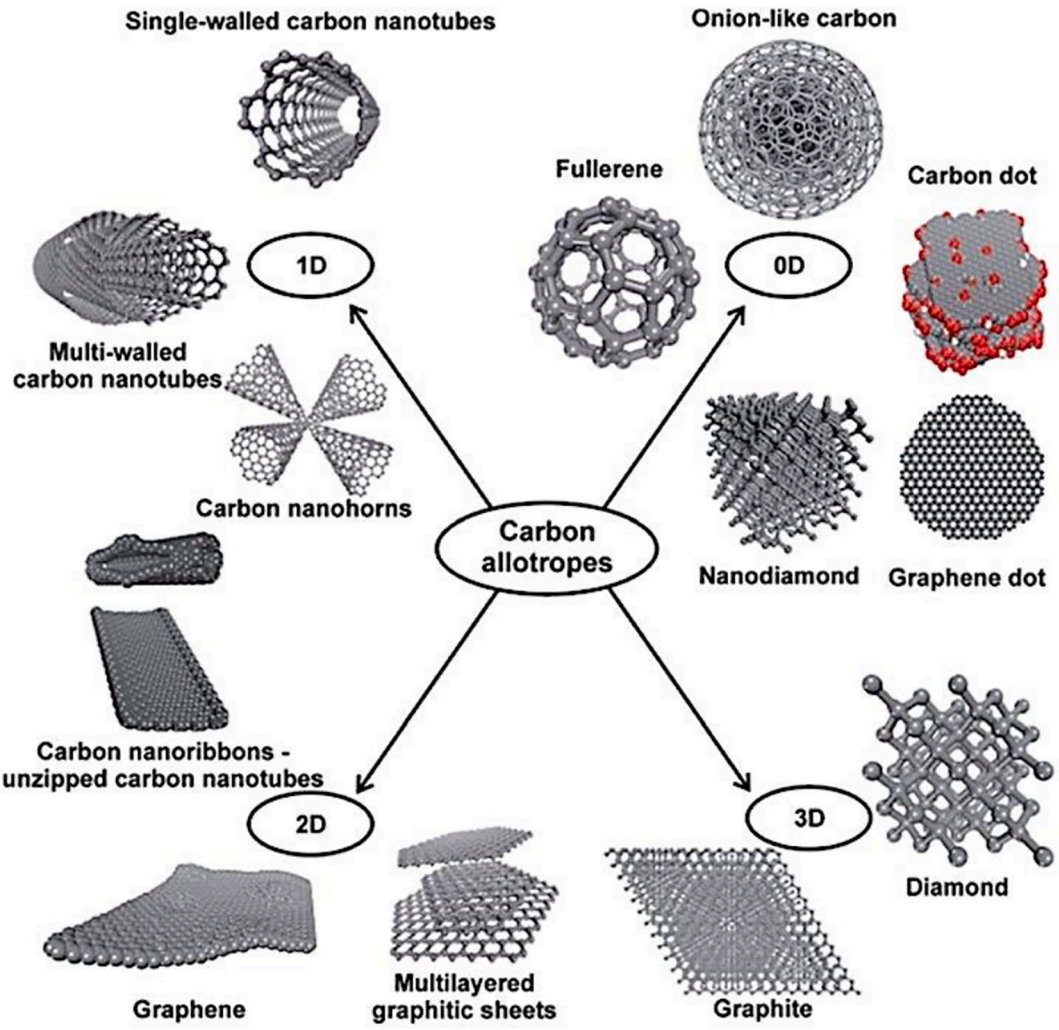

Fig. 7. Classification of carbon allotropes according to their dimensionality. Reproduced with permission [66]. Copyright 2019, Royal Society of Chemistry.

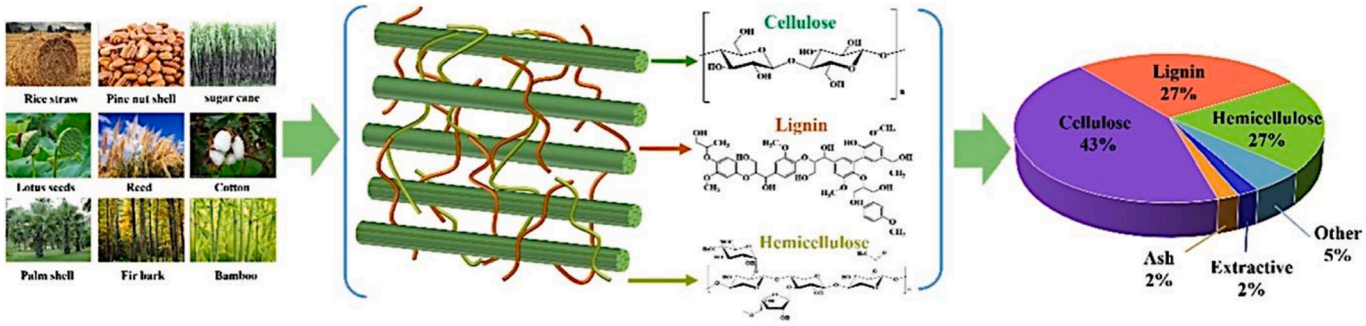

Fig. 8. Main structure and constituent distribution of typical biomass residues. Reproduced with permission [67]. Copyright 2022, Elsevier.

capacitance. Nitrogen is often the chosen doping element owing to its ease penetration into the carbon matrix with a specific capacitance of 278 F/g deliberated at a current density of 2 A/g when a N-doped interconnected porous carbon was prepared from flour food residue [69]. Chen and co-workers proposed a strategy for simultaneous carbonization, activation, and heteroatom doping of N and P onto the pomelo peel (carbon source). Impressively, co-doping N and P atoms induces more active sites and pore structure that gave rise to excellent capacitive and cyclic performances, as shown in Fig. 9 [70], implies the importance of pore engineering for the facilitation of electrolyte ions. The pore characteristic of activated carbon is dependent on the activation temperature where low activation temperature resulted in the formation of mesopores, and micropores at higher activation temperature. Doping sulfur onto the durian peels-derived AC resulted in a more ordered and condensed AC framework upon the evaporation of sulfur at high activation temperature, gave rise to the formation of micropores that could enhance the charge storage capacity of the S-doped AC [71].

Apart from energy storage, the S-doped carbon nanosheets derived from peanut root nodules exhibited remarkable electrocatalytic activity for HER in 0.5 M H_2SO_4 with a low onset potential of −0.027 V. DFT calculations verified that the S-atom interacts well with H^+ rather than the carbon atom due to the lone pair electrons, thus stabilizes the H*

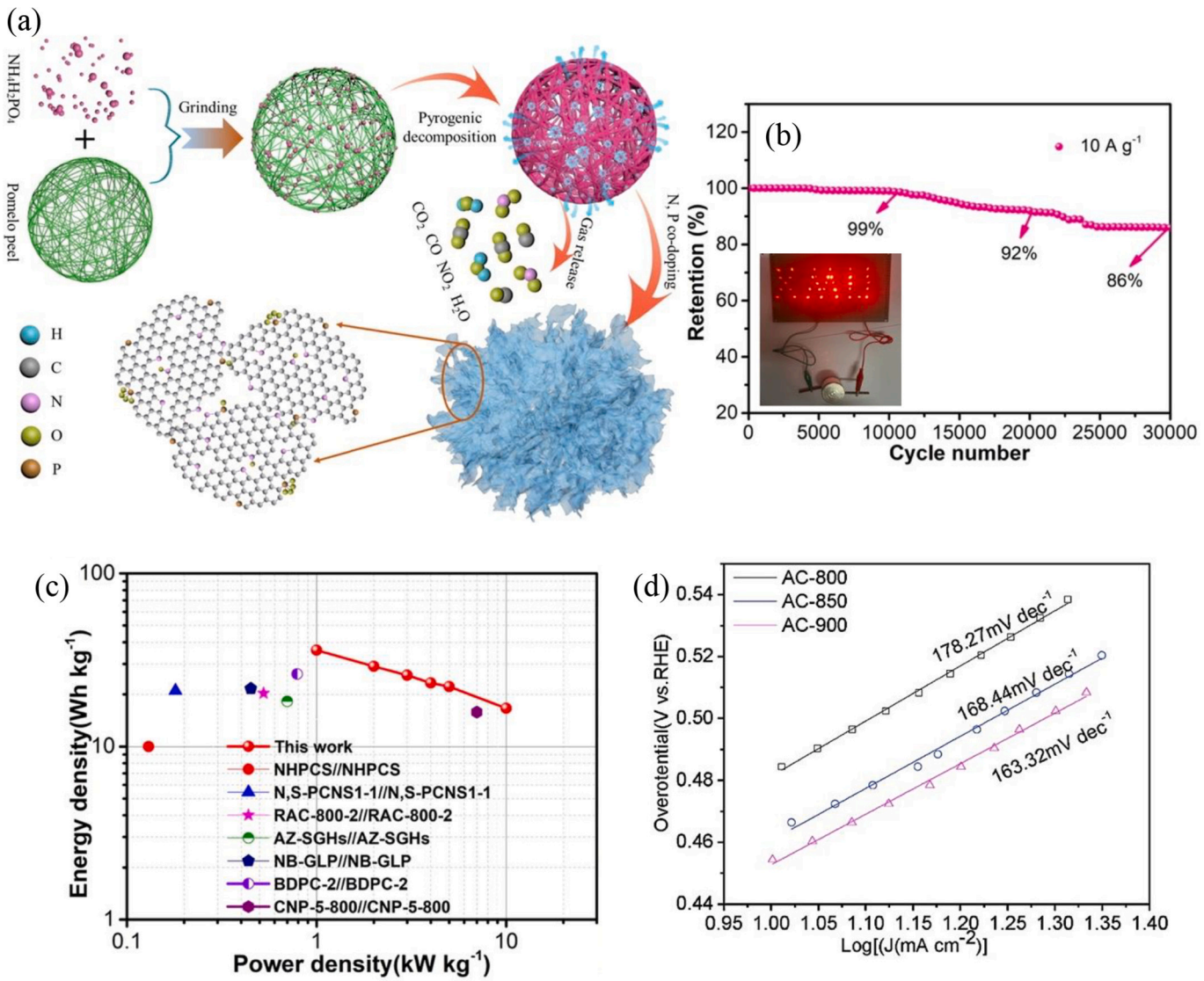

Fig. 9. (a) Illustration for the synthesis process of NPCNs. (b) cycling performance at a current density of 10 A/g, and (c) ragone plot of the NPCNs-750//NPCNs-750 SSC. Reproduced with permission [70]. Copyright 2022, Elsevier, and (d) Tafel plots of ACs for HER. Reproduced with permission [72]. Copyright 2020, Elsevier.

species in HER than the N-doping [73]. Thiopene, p-toluenesulfonic acid, and benzyl disulphide are the sulfur-containing organic compounds that have been used as the precursors of ACs where these compounds such as the thiophene sulfur stabilizes the active sites in the carbon lattice, leading to a low overpotential of 97 mV at 10 mA/cm^2 in the HER activity. When polystyrene sulfonate acid was used as the precursor for S-doped AC synthesis via pyrolysis at 900 °C, it was expected that some sulfonic acid groups were embedded in the carbon matrix as thiophene sulfur and sulfones, thus resulted in an efficient Volmer dynamics HER process with a Tafel slop of 163.32 mV/dec (Fig. 9d), suggesting S is a potential dopant to promote HER performance [72].

3.1.2. *Second and third-generation carbon materials*

Carbon nanofiber (CNF) is a 1D carbon material that have been widely explored for optoelectronics, energy storage, and environmental remediation. CNF possess smooth, porous, hollow, and stacked up structure, accompanied with high specific surface area, excellent thermal and electric conductivity, making them potential CNF-based functional nanomaterials. CNF is producible by electrospinning, CVD, and templated synthesis. Among them, electrospinning is the simplest fabrication method of all because CNF can be easily obtainable via high temperature carbonization after electrospinning the polymer (cellulose, chitin, lignin, and chitosan) nanofibers onto a substrate. For instance, Chen et al. fabricated a novel HER electrocatalyst composed of iron-doped cobalt phosphide porous carbon nanofibers, in short denoted as Fe-CoP/PCNF (**Fig. 10**a), via electrospinning, carbonization, and phosphorization (Fig. 10b). The resulted porous Fe-CoP/PCNF is larger in surface area than the Fe-CoP/CNF, accompanied with mesopores and macropores (Fig. 10c) that favour the electrolytes and gases diffusion during the HER process, attributed to PVP decomposition induced more pores during the carbonization process [74]. As depicted in Fig. 10d, pore forming agents (porogens) are usually included during the electrospinning process, and vaporizes during the heating treatment, leading to the formation of open holes. By comparing the electrode of polymer electrolyte membrane fuel cell (PEM) composed of Pt/CNF and Pt/C (platinum supported on carbon black), the Pt/CNF electrode is outperforming the Pt/C and establishes better stability owing to CNF possess an open structure that allows the exposure of catalyst particles to the reagents. Whilst, carbon black per se although featuring high specific surface area and high conductivity, however, its performance is usually compensated with easy oxidation of carbon into surface oxide and CO_2 with limited mass transfer [75].

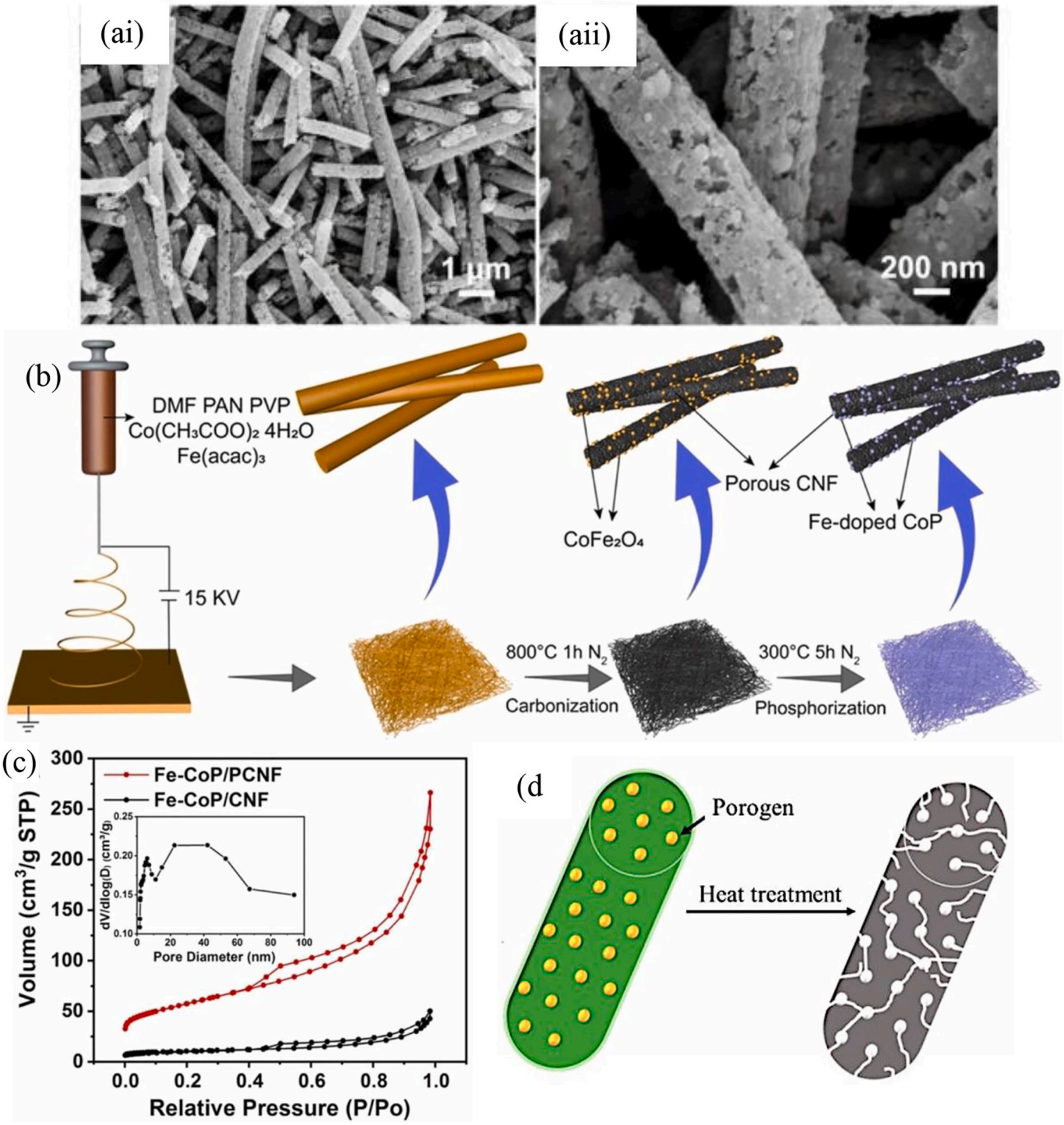

Fig. 10. (a) SEM image of Fe-CoP/PCNF, (b) schematic illustration of the fabrication of Fe-CoP/PCNF, and (c) nitrogen adsorption-desorption isotherm of Fe-CoP/PCNF and Fe-CoP/CNF. Reproduced with permission [74]. Copyright 2022, Elsevier, (d) pore-forming mechanism by a heat treating porogen. Reproduced with permission [75]. Copyright, 2023, American Chemical Society.

3.1.3. Fourth-generation carbon materials

The 2D graphene has proven itself as an efficient photocatalyts or cocatalyst for efficient photocatalytic H_2 production due to the available interfacial active sites for H^+ adsorption, rapid electron transfer, and excellent electrical conductivity. In addition, various materials were introduced onto the graphene surface and used as the multifunctional catalysts for an improved H_2 production rate. Nevertheless, the dispersion of the powder catalyst during synthesis and reaction is always the existing challenges that resulted in poor accessibility of electrons, electrolytes ions, and reactants diffusion due to the restacking of graphene sheets. Engineering 3D graphene network provides a new solution to the restacking issue of graphene sheets. The introduction of organic or linker molecule or metal oxides serves as the intercalation agent to prevent the restacking graphene sheets and create new functionalities through the cross interaction. Thanks to the porous, ample active sites and catalytic centers (large surface area) of the 3D graphene, this 3D network promotes light absorption and efficient charge transport pathway and diffusion.

Metal oxides (MOs) such as TiO_2 and ZnO_2 are the promising HER photocatalysts, but their current performance are limited by the large bandgap behaviour that has weaken the light absorption efficiency. Indirectly, higher energy are needed to excite the valence band electrons. To overcome the aforementioned problems, grafting graphene is regarded as an effective approach for visible light promotion. A graphene hydrogel composed of graphene sheets, TiO_2 nanorods, and 8 wt % Au nanoparticles has demonstrated an enhanced photocatalytic HER activity of 242 $\mu molh^{-1}\ g^{-1}$, which is 1.5-fold higher than the pristine TiO_2 nanorods (156 $\mu molh^{-1}\ g^{-1}$) and 4.7-fold higher than the 2D RGO-TiO_2 (51 $\mu molh^{-1}\ g^{-1}$) under UV–Vis light illumination, as shown in Fig. 11a. The outperforming Au/RGO-TiO_2 hydrogel is credited to the efficient electron transport pathway from Au to conduction band of TiO_2 due to the localized surface plasmon resonance effect, subsequently transferred to graphene to reduce H^+ to H_2 (Fig. 11b) [76,77]. Similarly, a RGO/ZnO composites demonstrated an improved photocatalytic activity and stability. Although MOs/graphene composite exhibited excellent properties for photocatalysis, however, the photocatalytic performance is still restrained by the poor electron storage capacity of the MOs/graphene composite. An europium (Eu)-TiO_2/graphene composite was investigated for photocatalytic H_2 production and results showed that the photocatalytic activity of the Eu doped composite was improved, as compared to the pristine TiO_2 [78]. The incorporation of ZnS enhances the absorbance of the ZnO-ZnS/graphene photocatalyst. Whilst the graphene sheet reduces interface resistance and promotes the absorption curve tail within the UV and visible light region, leading to an excellent H_2 evolution rate of 1070 $\mu molh^{-1}\ g^{-1}$ when ZnO-ZnS/graphene is up to an optimum weight ratio of 0.05 (Fig. 11c). Fig. 11d shows that the ZnS-ZnO heterostructure accelerates the electron-hole pairs separation, followed by the transferred of photogenerated electrons to the graphene for H^+ reduction [79].

Concerning the typical carbon nanomaterials derived from biomass or non-biomass compounds such as the AC and BC, they suffer several intrinsic drawbacks such as low surface area, poor pore connectivity, and poor morphological control because these carbon materials usually exist in bulk form. To synthesize carbon nanomaterials that fulfill the essential criteria mentioned above (surface area, porous structure, and unique morphology), carbon nanostructures of low-dimensions such as 1D fibrous and tubular structures, 2D nanosheets-like structures, and 3D micro−/nanostructures could be the best remediation, and these materials have been widely applied in energy storage, energy conversion, and electrocatalysis. Apart from the biomass-derived chars and non-biomass-chars composed of sewage sludge and waste tires, as mentioned above, the high carbon content of plastic waste makes them (plastic waste) a promising source or precursor for the synthesis of carbon nanomaterials. The potential value-added recovery of plastic waste offers interesting possibilities from an economic and environmental perspective rather than solely recycling them at higher cost expense. In most cases, plastic waste, in particular PP, PE, PS, and their mixture, have displayed their superior potential that would be carbonized and molded into different dimensionalities such as 1D nanotubes, 2D graphene sheets, and 3D nanostructures [80].

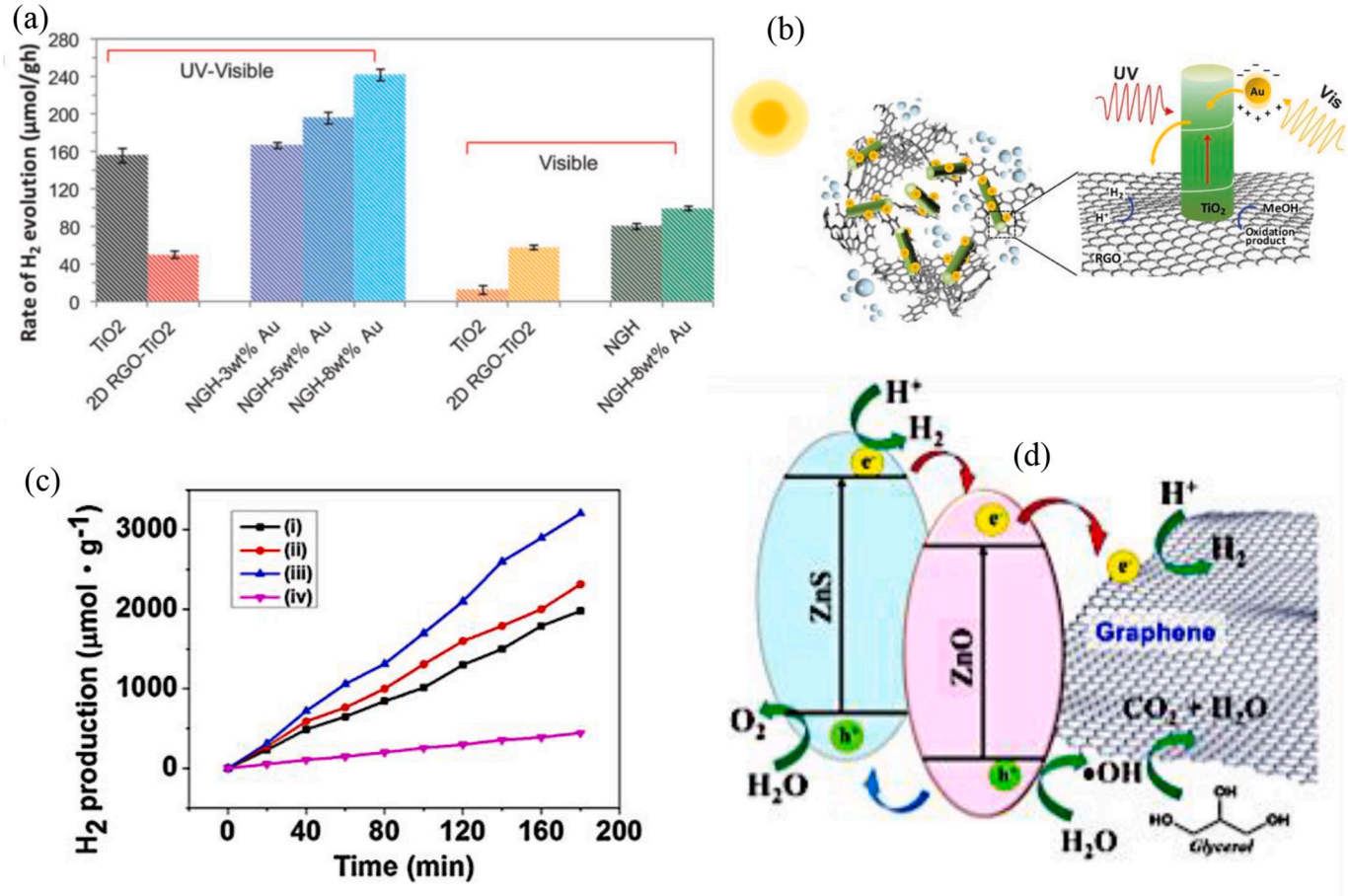

Fig. 11. Photocatalytic H_2 production studies of various samples. (a) H_2 production of the control samples (pure TiO_2 nanorods and 2D RGO-TiO_2 composite) and NGH with different wt% loading of Au nanoparticles under different light wavelength irradiations. (b) Proposed photocatalytic mechanism of the NGH-Au under ultraviolet and visible light irradiation. Reproduced with permission [77]. Copyright 2020, Wiley. (c) The amount of produced hydrogen by (i) ZG0 (ii) ZG1 (iii) ZG5 and (iv) ZG10 photocatalysts prepared at different graphene/ZnO-ZnS weight ratio during 3 h irradiation, and (d) illustration of water splitting and glycerol oxidation/reforming reactions over the ZnO-ZnS/graphene photocatalyst under light irradiation. Reproduced with permission [79]. Copyright 2018, Elsevier.

For example, the production of CNTs by pyrolysis-catalysis of plastics has become an attractive idea to researchers as an effort of one stone killing two birds in solving the plastic waste-related issues and upcycling the waste to get value-added products. The CNT growth mechanism is complex, and it varies with different feedstocks and the process conditions such as the reaction temperature and reactors. The precursors' molecular structure directly affects the morphology of CNTs, where linear structured CNTs are derived from linear hydrocarbons. While cyclic hydrocarbons result in curved CNT formation with bridges inside the tubes [81]. The formation of SWCNT occurs at a higher temperature than that of MWCNTs, which is 600–900 °C and 900–1200 °C, respectively [10,12]. The influence of temperature on MWCNTs derived from PP via a pyrolysis catalytic-reforming process was investigated by Liu et al., and they found that the optimum temperature for MWCNT formation was at 700 °C [82]. In another work, high-value CNTs and hydrogen co-production were produced from the two-stage pyrolysis-catalytic reforming/gasification of waste tires over Ni/Al_2O_3, Co/Al_2O_3, Fe/Al_2O_3, and Cu/Al_2O_3 as the catalysts at 600–800 °C. Results showed that Ni/Al_2O_3 catalyst produced high-quality MWCNTs and the highest H_2 yield than the other catalysts, which implies the choice of catalysts partake in the quality of carbon produced [83]. Using Ni as the catalyst, Lisak and co-workers showed that temperature is the main factor influencing the quality of CNTs of this work. Mixed plastics (LDPE, PP, PS, and PET) are decomposed via pyrolysis, and the non-condensable pyrolysis gases are further converted into functional MWCNTs through chemical vapor deposition using Ni-based catalyst at a temperature of 500 and 800 °C [11]. CNTs produced at lower temperatures behave as superior electrocatalysts in oxygen reduction reaction (ORR) owing to a higher density of edge defects in carbon nanomaterials that provide ample active sites for electrocatalytic reactions. The availability of edge defect sites for the case of ORR allows heterogeneous electron transfer from the electrode into the electrolyte [84]. Likewise, when it is the case for thermochemical conversion, it is postulated that the formation of these defective active sites allows the adsorption of reactants for catalytic reactions to take place.

3.2. Environmental remediation

The disposal of non-treated wastewater from the textile and chemicals industries into waterways has stirred severe environmental issue. Among the various reported conventional methods (physical, chemical, and biological), catalytic adsorption is regarded as one of the most effective approaches to remove synthetic dyes and heavy metals by using inexpensive nano-adsorbents such as activated carbon, graphene, carbon nanotubes, etc. because these carbonaceous materials have been recognised as the best technologies for water decolorization by the US Environmental Protection Agency [85]. The adsorption efficiency is relying on the physisorption and chemisorption processes between the catalyst (adsorbent) and pollutants. Thus engineering the strong oxidizing radicals/free bonds on the adsorbent are important to attract the incoming pollutants through the formation of interactions (hydrogen bonding, hydrophobic interactions, polar-π interactions, electrostatic interaction, and aromatic interactions, as depicted in Fig. 12.

3.2.1. First-generation carbon materials

AC is one of the most widely used adsorbents for organic/dyes and heavy metals removal owing to its ease availability and excellent properties (resistive to acid/base, corrosion, extreme temperatures, and biocompatibility). The AC deriving from either biomass (coconut husk, sugarcane bagasse, etc.), mineral raw materials (bituminous coal, peat, etc.), waste rubber, and waste plastic by high-temperature pyrolysis and activation are mouldable into various shapes/dimensions with favorable surface functions and textural carbon characteristics for pollutants adsorption [86]. The available surface functionalities such as -OH and

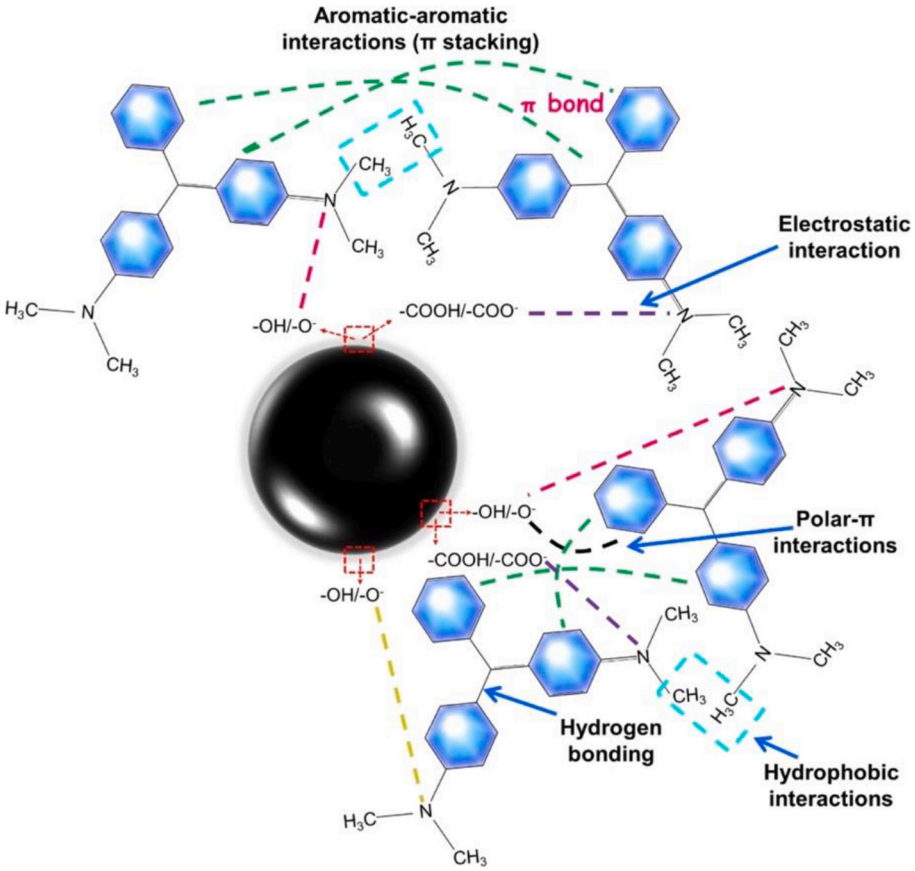

Fig. 12. The possible attraction forces for adsorption onto catalyst surface. Reproduced with permission [85]. Copyright 2021, Elsevier.

-COOH groups on AC serve as the active sites to bind the pollutants chemically or physically for removal. Further enhancing the adsorption capacity of AC can be performed through physical and chemical treatment such as carbonization and activation for pore engineering and chemical activating agents for chemical activation. An AC derived from lignin with $FeCl_3$ prepared by chemical activation using microwave heating was used to treat acetaminophen pollutant. Results show that the impregnation ratio and activation time are the main factors that guarding the porosity feature of the AC that could dramatically improve its adsorption capacity [87]. Rubber seed (RS) and rubber seed shells (*RSS*)-derived ACs in the powdered form (PACs) were prepared through carbonization, followed by KOH, NaOH, and H_2SO_4 activation for methylene blue dye removal. Results show that the NaOH-activated RSS-PAC and H_2SO_4-activated RS-PAC demonstrated the best adsorption capability, attributed to the pore size structure created by NaOH and the availability of hydroxyl, alkoxy, and carboxyl functional groups [88]. However, the powdered form AC is unfavorable because it is difficult to be collected from the medium, consequently cause secondary pollution. To solve the aforementioned issues, a novel binderless core-shell AC in the formed of granular was synthesized (PAC as the core and silica sol and wood powder as the shell) and exhibited the highest adsorption capacity of 113.2 mg/g, credited to the 3D open pore network structure of granular AC shell that strengthen the adsorption capability of adsorbates to the PAC core [89]. Apart from the activation method, pH is an another criterion to be considered for adsorption capacity. The adsorption capacity of malachite green (MG) dye by P-aminobenzoic acid-functionalized AC was improved from pH 2–7, ascribed to the reduction of positive charge density on the catalyst's surface sites that enhances electrostatic and π-π interactions, thereby improved the adsorption efficiency. Controlling the pH is importance because an acidic medium may resulted in the competition between hydronium ions and MG cations for the active sites. Whilst, a basic medium may change the MG structure and resulted in poor adsorption capacity [90].

3.2.2. Second and third-generation carbon materials

The emerging exfoliated graphite (EG) has received considerable attention to date owing to its excellent mechanical, electrical, thermal, and dielectric properties. However, the synthesis process of EG is tedious (multiple steps required), time and chemicals consuming, and the final amount obtained is low. EG is conventionally synthesized using H_2SO_4/HNO_3/$HClO_4$ as the spacing agent and $KMnO_4$/ammonium persulphate/hydrogen peroxide as the oxidizing agent, followed by conventional or microwave heating, which hike the overall production (time and cost). Hence, exploring a more simpler, large scale, and cost effective methods to produce high quality and quantity EG is called for action. An expanded graphite modified by CTAB-KBR/H_3PO_4 was synthesized using CTAB/KBr and natural flake graphite as the intercalation agents, and H_3PO_4 for activation at low temperature. The modified EG is highly hydrophobic, as evidenced through water contact angle (WCA) measurement where the EG recorded a WCA of 129°, whereas WCA of 135.6° was recorded for the modified EG (**Figs. 13**a-b), and shown good engine oil absorption under high salinity conditions. Exhibited excellent oil adsorption ability and reusability (Fig. 13c) [91]. Similarly, a CTAB-modified graphite was employed to investigate the adsorption behaviour of BPA [92]. The key point of this research revealed that the CTAB concentration and the incubation time are the important parameters to be optimized for BPA adsolubilization. Fig. 13d shows that the adsorption capacity of BPA increases with increasing CTAB concentration up to a maximum concentration of 9.5 mmol/L. Similar trend was observed in the incubation time plot (Fig. 13e) where the optimal incubation time was 24 h [92]. When γ-Fe_2O_3 was added to the EG, a magnetic highly porous (evidenced through SEM images in Figs. 13f-g) iron-containing EG was obtained in a two-step synthesis method . This magnetic macroporous absorbent managed to absorb vast amount of oil, hexane, octane, isopropanol, acetone, benzene, and toluene in an ultra-fast mode in seconds in the macropore volume (Fig. 13h). Thanks to the ferromagnetic properties in EG composition, the sorbent can be collected from water with a magnet, which open a new research direction on pollutant removal technology [93].

3.2.3. Fourth-generation carbon materials

The conventional microporous AC is usually suffering from poor adsorption issue for bulky compounds due to the size exclusion effect [94]. Alternatively, graphene oxide (GO) and its derivatives, whom possess high surface area of 2630 m^2/g, have been considered as ideal adsorbent for organic and dyes removal from industrial effluents, credited to its unique physical and chemical properties. The presence of surface oxygenated functional groups such as hydroxyl, carboxyl, carbonyl, etc., wrinkles, and the π-electron domains in the planar structure of rGO contributes to the adsorptive characteristics [95]. Surface complexation between positively charge metal ions and negatively charge oxygenated functional groups of graphene plays a pivotal role in Pb(II) adsorption, while the removal efficiency is dependent on the dye-absorbent interaction, nature of dyes, surface area and porosity of adsorbent, pH, etc. The pH of the solution should be carefully adjusted because pH affects the absorbents' surface charge and metal ionic species, in which H^+ and H_3O^+ would compete with metal ions for the available binding sites on graphene at low pH condition. On the other hand, deprotonation of oxygenated groups at high pH (high concentration of OH^-) resulted in poor absorption capacity. Temperature is an important factor to be optimized because an elevated temperature increases the sorption sites on the graphene surface and enhances the diffusion rate of the metal ion. Comparing GO and rGO, GO binds well with the positively charged metal ions via electrostatic attraction, ascribed to its abundant oxygenated groups (vary according to its graphite precursor). The adsorption capacity of amorphous graphite-derived GO (766.8 mg/g) is outperforming the flaky (746.2 mg/g) and lump (738.5 mg/g) graphite. The bare GO exhibited significant drawbacks for adsorptive performance due to restacking of GO sheets by Van der Waals interaction and limited affinity of bare GO toward anionic dyes and heavy metals [96]. Thus, GO surfaces were usually modified by exfoliation or doping with various inorganic, organic, and polymeric materials to overcome the aggregation issue for effective adsorptive performance. The coating of silicon dioxide (SiO_2) on the GO surface improved the affinity toward Pb(II) and As(III) metal ions. A sandwich-like GO@SiO_2@C@Ni composite was prepared by Molaei and co-workers for the removal of Cr(VI). Thanks to the hydrophilicity, stability, large surface area with vast functional groups available on the GO@SiO_2@C@Ni composite, the synergistic effects between each material favors the Cr(VI) adsorption [97]. Instead, using an organic polymer as the additive is more effective in metal ions adsorption than an inorganic composite owing to the presence of chelating groups. Typically, the polymers with nitrogen containing group such as polyaniline, polyethylenimine and polypyrrole have proven their effectiveness in excellent metal ions adsorption [98,99]. For instance, a magnetic polypyrrole-graphene oxide composites exhibited high Hg(II) removal rate of 400 mg/g at pH 7, attributed to the strong electrostatic attraction between negatively charged chelating agents and positively charged Hg (II) [100]. Likewise, when poly(allylamine hydrochloride) was coated on GO (PAH-GO), the available amino groups of PAH binded to the Cu (II), thereby contributed to a high Cu(II) adsorption capacity of 349.03 mg/g at pH 6 [101].

Because porosity and surface area are the main keywords for a catalyst, catalyst regeneration/reusability is also crucial for a catalysis reaction. It is always challenging to separate the catalyst from water through filtration for reuse. [102] Hence, the research focus has now steering toward carbon-based nanostructures with the separation capability of magnetic nanomaterials. Ferromagnetic ceramic material, namely cobalt ferrite ($CoFe_2O_4$), renders high magnetic crystal anisotropy and coercivity, medium saturation magnetization, and physically/chemically stable, making them promising magnetic materials. Using

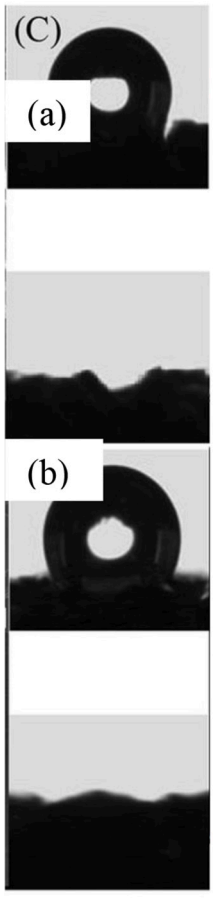

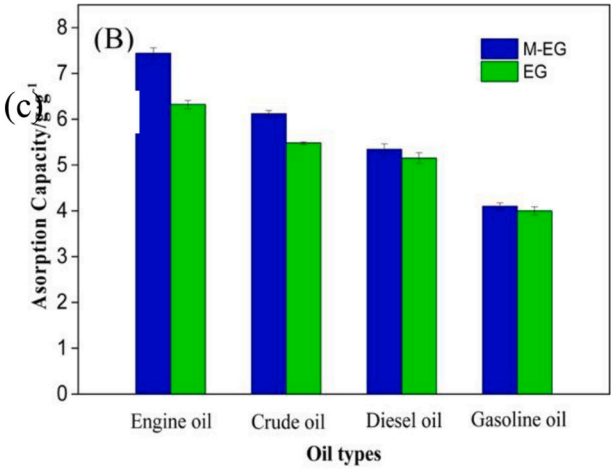

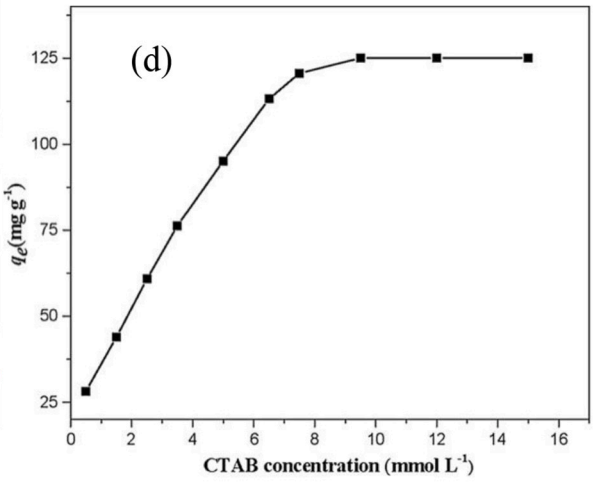

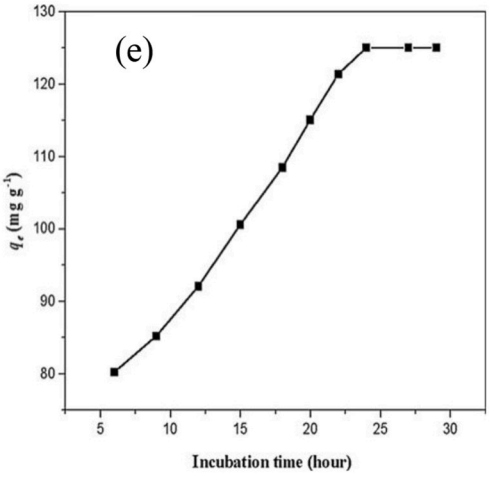

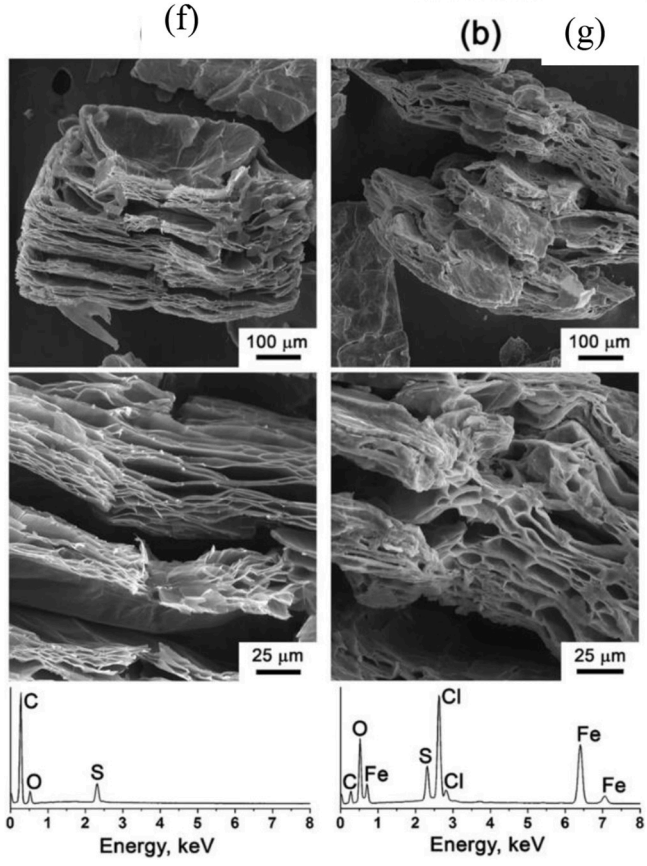

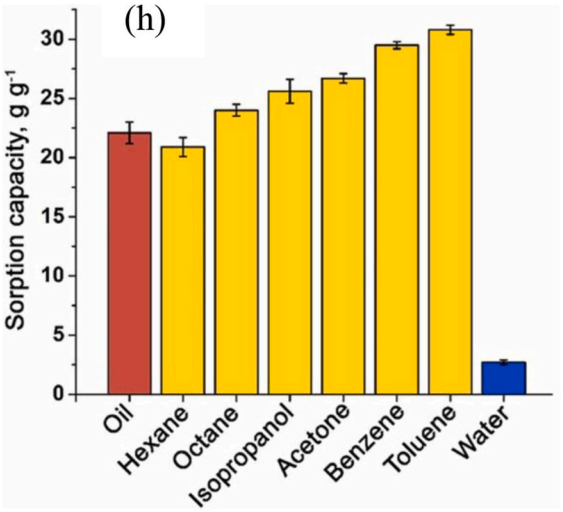

(caption on next page)

Fig. 13. Wettability measurement of (a) EG and (b) modified EG, (c) marine oil types effect on the removal performance by modified EG and EG. Reproduced with permission [91]. Copyright 2018, Elsevier. Effects of (d) CTAB concentration and (e) incubation time on BPA adsorption. Reproduced with permission [92]. Copyright 2018, Elsevier. SEM images and EDX spectra of (f) initial expandable graphite and (g) expandable graphite impregnated in the $FeCl_3$ solution, and (h) sorption capacity of EG_{Fe}-1000 toward different liquids. Reproduced with permission [93]. Copyright 2023, Elsevier.

$CoFe_2O_4$ as the prime magnetic contributor, Kamali and co-workers mixed PET with iron, cobalt oxides, and sodium chloride salt to produce the magnetic dye adsorbent agents (Fig. 14a) that possesses an excellent magnetic performance of 17.9 emu/g and dye adsorption capacity for methylene blue of 277.78 mg/g and methylene orange (238.09 mg/g). [103] The magnetic property of the catalyst enables quick and efficient separation from the water mixture by applying an external magnetic field, giving rise to a high adsorption capacity of >95% of its original capacity after six cycles of regeneration. Specifically, the process involves ball-milling of Fe_2O_3 and CoO in the presence of n-hexane in forming Fe_2O_3/CoO/Co_3F_7 nanostructured, followed by the molten salt treatment of ball-milled samples with PET plastics waste to form Co_3Fe_7/$CoFe_2O_4$ embedded on graphitic carbon matrix. The formation of mesoporous carbon nanostructures (MCN) is attributed to the carbonization of PET during the heat-treatment process. It has demonstrated that the interaction between graphite and plastic-derived carbons with molten salts formed carbon nanostructures with a higher degree of graphitization and specific electrical conductivity values. [104] The successful development of the porous ternary nanostructure was demonstrated by SEM (Fig. 14b) and EDX elemental mapping (Fig. 14 ci-iv), displaying the homogeneous distribution of C, Co, Fe, and O elements.

The significant findings and advantages of appointing magnetic-based carbon nanomaterials as the adsorbent have been emphasized and being highlighted recently. Apart from magnetic carbon derived from plastic waste, as described above, novel and robust magnetic N-doped nanocarbon springs synthesized through one-pot solid pyrolysis were reported by Kang et al. [105] In this work, the carbon material is not composed of plastic waste. Mn@NCNTs catalysts were developed by direct thermal pyrolysis of melamine with $MnCl_2$, using Mn nanoparticles as the catalysts at 800 °C to convert amorphous carbon into graphitic carbons, as shown in Fig. 15a. The graphite cages serve as building blocks for the growth and formation of CNTs from the tip of Mn nanoparticles, while the Mn/C clusters are gradually consumed and bonded in the stable form of CNTs and Mn_7C_3. After that, acid treatment was performed to remove the superficial metals and oxides, leaving the open-ended and hollow helical tubes of CNTs. The SEM image (Fig. 15b) shows a smooth spring-like morphology of Mn@CNTs-800 with 3–5 μm in length and 20–40 nm in ring diameter, and the hollow tubing structure with an inner tunnel diameter of ~20 nm was explicated by TEM image in Fig. 15c. These magnetic nanohybrids were applied for peroxymonosulfate activation for the first time to generate highly oxidizing radicals for the decomposition of microplastics under hydrothermal conditions. These robust carbon hybrids with spiral architecture and highly graphitic degree guaranteed superb stability in the hydrothermal environment. This work opens a new pathway for the synthesis of carbon catalysts by merging state-of-the-art carbocatalysis and nanotechnology to remediation of microplastics contamination in water.

In summary, rationally transforming plastic waste into helpful carbon nanomaterials with special dimensionalities and morphologies can be applied in thermocatalysis such as plastic upcycling because lower dimension carbon materials present surface defects that act as active sites for catalytic reactions. This section aims to enlighten the readers with the challenges and the most significant potential of different dimensional plastic-derived carbon materials as green carbon catalysts for thermochemical application. To the best knowledge that we have, the carbon catalysts used in thermochemical conversion to date are mainly confined to bulk AC and char-based materials, which have limited their practical applications due to dissatisfactory conversion efficiency, poor surface area, and pore connections. Hence, we propose the importance of the rational design of carbon catalyst, especially using plastic waste as the carbon feedstock for the reasons of (i) plunging the

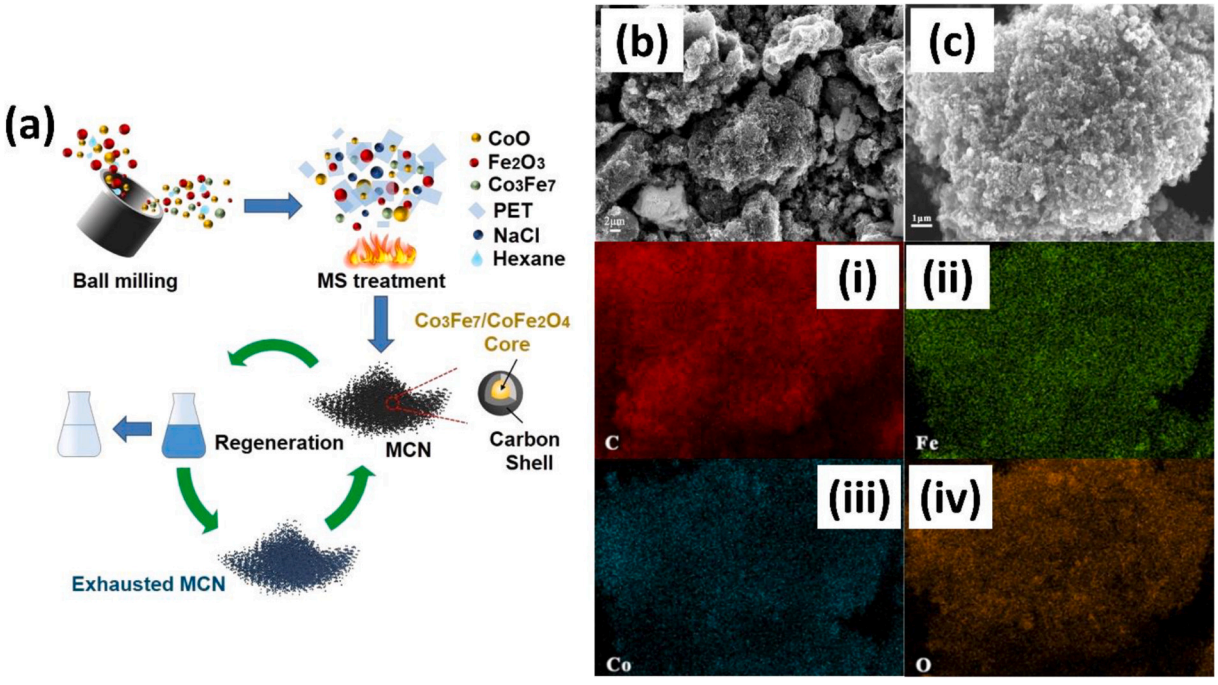

Fig. 14. (a) Schematic illustration of the method used for the fabrication of the magnetic carbon nanostructure, (b) representative SEM micrographs of the regenerated MCN after five cycles of adsorption/regeneration, and (c) SEM micrograph and the corresponding elemental mapping analysis of (i) C, (ii) Fe, (iii) Co, and (iv) O. Reproduced with permission [103]. Copyright 2021, Elsevier.

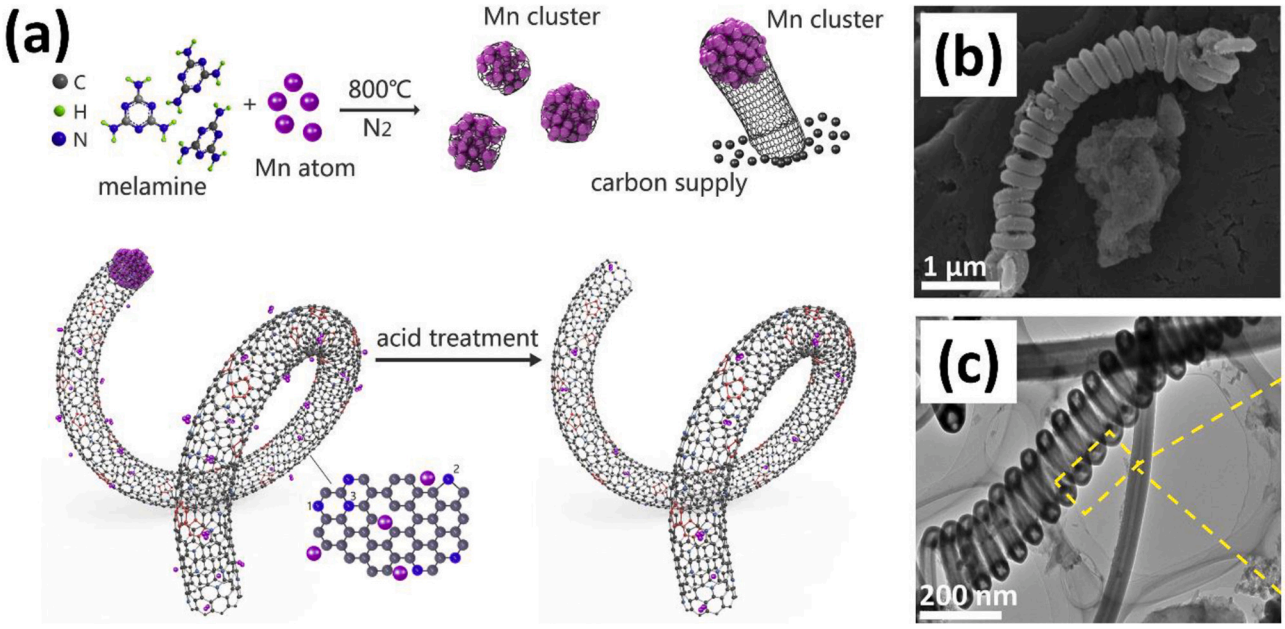

Fig. 15. (a) Schematic illustration of the procedure for the preparation of Mn@NCNTs preparation, (b) SEM image, and (c) TEM image of Mn@NCNTs-800. Reproduced with permission [105]. Copyright 2019, Elsevier.

accumulation of plastics waste (white pollution) and (ii) these unique carbon nanostructures would present a new research paradigm in plastic upcycling. In addition, magnetic-based nanomaterials as the catalysts have been significantly flourishing in catalysis, from the standpoint of catalysts regeneration and reusability because the catalysts can be easily separated from any mixtures, either water-based or solid-based, with the use of an external magnet, which is cost and time-saving in a sustainable manner. The explosive interests in the arena of magnetic-carbon catalysts indeed create a new stir in the catalysis context.

4. Conclusion and perspective

As a conclusion, the synthesis and fabrication strategies of carbonaceous nanomaterials derived from biomass, non-biomass, and plastic waste were first summarized, followed by their applications for energy and environmental remediation (Fig. 16). These carbonaceous nanomaterials are derivable through different methods, including HTC, template approaches, activation approaches, CVD, and carbonization, and the effects of synthesis routes toward the engineering of micro/mesoporous carbon structure, as well as their physical and chemical properties of the carbonaceous are disclosed in this review. The engineering of 3D carbon nanostructure in low dimensional, as well as the approaches to improve catalytic activity and adsorption ability through doping engineering (with metal and non-metal nanoparticles) are explored and explicated. The carbons' interconnected structure, high surface area and porosity structure making them efficient in mass transfer, mass diffusion and storage (accessible of electrolyte ions), thus have been widely used in energy storage and environmental science.

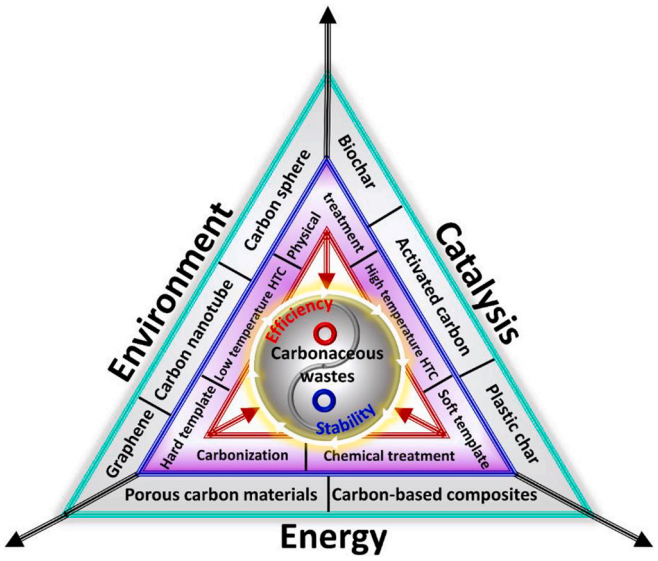

Fig. 16. Interrelationship of predominant factors in carbonaceous nanomaterials design for catalysis, energy, and environmental remediation toward sustainable manner.

Although the carbon research has been well-progressing, however, there are still challenges in their preparation for large scale application. Here are some potential studies that could be performed for energy and environmental applications. First, doping engineering has been performed to improve the catalytic performance of the carbon, however, the doping-induced enhancement at the atomic and molecular level has not been in-depth. Thus, simulation studies should be corroborated to understanding the catalytic reaction mechanism. Second, catalytic performance of the single atom catalyst-carbon hybrid system should be investigated, instead of solely focusing on the metal nanoparticles. Thus far, metal nanoparticles are widely employed in most reaction system, but in fact, both the nanoparticles and single atom catalyst exhibited own advantages where reasonable choice should be made according to the particular reaction and demand at the time [17]. Thirdly, most of the current experiments are laboratory scale basis. Thus, in order to promote large scale application, these carbon materials should be integrated into designated equipment for future research [18]. Lastly, carbon materials derived from plastic waste are emerging, but the performance of the plastic-derived carbon is somehow still underperforming, as compared to the biomass based derived carbon. This could be ascribed to the nature, composition of yield, and quality of the feedstocks (biomass and plastic waste). functional groups found in the raw precursor [106]. The biomass materials usually composed of high oxygen content elements which give rise to the production of highly oxygenated products, which is much useful in energy and environmental application such as the available functional groups to cling the pollutant from water source and

etc.. Contrarily, the synthetic polymeric materials possess lower oxygen concentration that has lesser or no functional groups available. Hence, *co*-processing biomass with synthetic polymers could be a viable method to balance the feedstock amount of carbon, oxygen, and hydrogen so as to improve the properties of the carbon materials.

We hope that this review article will be a good research guidebook for developing biomass/non-biomass carbonaceous-based nanomaterials in the future. We are confident that interdisciplinary research collaborations between the chemists, physicists, engineers, materials scientists will positively bring new findings and knowledge translation in materials science and technology, address the bottleneck of environmental-related subjects, and overcome the crisis of fossil fuel depletion through the production of innovative products for green and sustainable future.

CRediT authorship contribution statement

Chi Huey Ng: Conceptualization, Data curation, Formal analysis, Investigation, Validation, Visualization, Writing – original draft, Writing – review & editing. **Mohd Aizzan Mistoh:** Investigation, Methodology. **Siow Hwa Teo:** Conceptualization, Data curation, Formal analysis, Project administration, Resources, Supervision, Validation, Writing – original draft, Writing – review & editing. **Andrea Galassi:** Methodology. **Yun Hin Taufiq-Yap:** Conceptualization, Funding acquisition, Project administration, Supervision. **Nancy Julius Siambun:** Investigation. **Jurry Foo:** Validation. **Coswald Stephen Sipaut:** Software, Validation. **Jeffrey Seay:** Supervision. **Jidon Janaun:** Funding acquisition, Supervision.

Declaration of competing interest

The authors declare that they have no known competing financial interests or personal relationships that could have appeared to influence the work reported in this paper.

Data availability

No data was used for the research described in the article.

Acknowledgements

This research was supported by the Universiti Malaysia Sabah Special Grant Scheme (SDK0321-2021) and the Ministry of Higher Education Malaysia Translational Research (TR@M).

References

[1] R. Rauti, M. Musto, S. Bosi, M. Prato, L. Ballerini, Properties and behavior of carbon nanomaterials when interfacing neuronal cells: how far have we come? Carbon. 143 (2019) 430–446.
[2] J. Miao, Z. Lang, T. Xue, Y. Li, Y. Li, J. Cheng, H. Zhang, Z. Tang, Revival of zeolite-templated Nanocarbon materials: recent advances in energy storage and conversion, Adv. Sci. 7 (2020) 2001335.
[3] X. Gao, H. Liu, D. Wang, J. Zhang, Graphdiyne: synthesis, properties, and applications, Chem. Soc. Rev. 48 (2019) 908–936.
[4] A.M. Dehkhoda, A.H. West, N. Ellis, Biochar based solid acid catalyst for biodiesel production, Appl. Catal. A Gen. 382 (2010) 197–204.
[5] J.S. Cha, J.C. Choi, J.H. Ko, Y.K. Park, S.H. Park, K.E. Jeong, S.S. Kim, J.K. Jeon, The low-temperature SCR of NO over rice straw and sewage sludge derived char, Chem. Eng. J. 156 (2010) 321–327.
[6] B. Hu, K. Wang, L. Wu, S.H. Yu, M. Antonietti, M.M. Titirici, Engineering carbon materials from the hydrothermal carbonization process of biomass, Adv. Mater. 22 (2010) 813–828.
[7] M. Bahri, S.H. Gebre, M.A. Elaguech, F.T. Dajan, M.G. Sendeku, C. Tlili, D. Wang, Recent advances in chemical vapour deposition techniques for graphene-based nanoarchitectures: from synthesis to contemporary applications, Coord. Chem. Rev. 475 (2023) 214910.
[8] D.T. Oyekunle, X. Zhou, A. Shahzad, Z. Chen, Review on carbonaceous materials as persulfate activators: structure–performance relationship, mechanism and future perspectives on water treatment, J. Mater. Chem. A 9 (2021) 8012–8050.
[9] M.A. Ahmed, A.A. Mohamed, Recent progress in semiconductor/graphene photocatalysts: synthesis, photocatalytic applications, and challenges, RSC Adv. 13 (2023) 421–439.
[10] M. Kumar, Y. Ando, Chemical vapor deposition of carbon nanotubes: a review on growth mechanism and mass production, J. Nanosci. Nanotechnol. 10 (2010) 3739–3758.
[11] J.G.S. Moo, A. Veksha, W. Da Oh, A. Giannis, W.D.C. Udayanga, S.X. Lin, L. Ge, G. Lisak, Plastic derived carbon nanotubes for electrocatalytic oxygen reduction reaction: effects of plastic feedstock and synthesis temperature, Electrochem. Commun. 101 (2019) 11–18.
[12] Y.S. Zhang, H.L. Zhu, D. Yao, P.T. Williams, C. Wu, D. Xu, Q. Hu, G. Manos, L. Yu, M. Zhao, P.R. Shearing, D.J.L. Brett, Thermo-chemical conversion of carbonaceous wastes for CNT and hydrogen production: a review, Sustain. Energy & Fuels 5 (2021) 4173–4208.
[13] D. Chu, H. Dong, Y. Li, J. Xiao, X. Hou, S. Xiang, Q. Dong, Sulfur or nitrogen-doped rGO supported Fe-Mn bimetal–organic frameworks composite as an efficient heterogeneous catalyst for degradation of sulfamethazine via peroxydisulfate activation, J. Hazard. Mater. 436 (2022) 129183.
[14] J. Liu, J. Jiang, M. Wang, J. Kang, J. Zhang, S. Liu, Y. Tang, S. Li, Peroxymonosulfate activation by cobalt particles embedded into biochar for levofloxacin degradation: efficiency, stability, and mechanism, Sep. Purif. Technol. 294 (2022) 121082.
[15] Q. Shi, S. Deng, Y. Zheng, Y. Du, L. Li, S. Yang, G. Zhang, L. Du, G. Wang, M. Cheng, Y. Liu, The application of transition metal-modified biochar in sulfate radical based advanced oxidation processes, Environ. Res. 212 (2022) 113340.
[16] Z. Yang, J. Qian, A. Yu, B. Pan, Singlet oxygen mediated iron-based Fenton-like catalysis under nanoconfinement, Proc. Natl. Acad. Sci. 116 (2019) 6659–6664.
[17] H. Ou, D. Wang, Y. Li, How to select effective electrocatalysts: Nano or single atom? Nano Select. 2 (2021) 492–511.
[18] H. Yan, C. Lai, S. Liu, D. Wang, X. Zhou, M. Zhang, L. Li, X. Li, F. Xu, J. Nie, Metal-carbon hybrid materials induced persulfate activation: application, mechanism, and tunable reaction pathways, Water Res. 234 (2023) 119808.
[19] E. Lam, J.H.T. Luong, Carbon materials as catalyst supports and catalysts in the transformation of biomass to fuels and chemicals, ACS Catal. 4 (2014) 3393–3410.
[20] Y. Shen, A review on hydrothermal carbonization of biomass and plastic wastes to energy products, Biomass Bioenergy 134 (2020) 105479.
[21] R.I. Walton, Subcritical solvothermal synthesis of condensed inorganic materials, Chem. Soc. Rev. 31 (2002) 230–238.
[22] G.R. Patzke, F. Krumeich, R. Nesper, Oxidic nanotubes and nanorods—anisotropic modules for a future nanotechnology, Angew. Chem. Int. Ed. 41 (2002) 2446–2461.
[23] M.T. Reza, M.H. Uddin, J.G. Lynam, S.K. Hoekman, C.J. Coronella, Hydrothermal carbonization of loblolly pine: reaction chemistry and water balance, Biomass Conver. Biorefin. 4 (2014) 311–321.
[24] Z.E. Tang, S. Lim, Y.L. Pang, H.C. Ong, K.T. Lee, Synthesis of biomass as heterogeneous catalyst for application in biodiesel production: state of the art and fundamental review, Renew. Sust. Energ. Rev. 92 (2018) 235–253.
[25] R. Gamgoum, A. Dutta, R. Santos, Y. Chiang, Hydrothermal conversion of neutral sulfite semi-chemical red liquor into Hydrochar, Energies. 9 (2016) 435.
[26] J. Fang, L. Zhan, Y.S. Ok, B. Gao, Minireview of potential applications of hydrochar derived from hydrothermal carbonization of biomass, J. Ind. Eng. Chem. 57 (2018) 15–21.
[27] B. Szczęśniak, J. Phuriragpitikhon, J. Choma, M. Jaroniec, Recent advances in the development and applications of biomass-derived carbons with uniform porosity, J. Mater. Chem. A 8 (2020) 18464–18491.
[28] Y. Qi, M. Zhang, L. Qi, Y. Qi, Mechanism for the formation and growth of carbonaceous spheres from sucrose by hydrothermal carbonization, RSC Adv. 6 (2016) 20814–20823.
[29] Y. Zhang, W. Hou, H. Guo, S. Shi, J. Dai, Preparation and characterization of carbon microspheres from waste cotton textiles by hydrothermal carbonization, J. Renew. Mater. 7 (2019) 1309–1319.
[30] G. Wang, H. Xu, L. Lu, H. Zhao, One-step synthesis of mesoporous MnO_2/carbon sphere composites for asymmetric electrochemical capacitors, J. Mater. Chem. A 3 (2014) 1127–1132.
[31] C. Lamiel, V.H. Nguyen, M. Baynosa, D.C. Huynh, J.J. Shim, Hierarchical mesoporous carbon sphere@nickel cobalt sulfide core-shell structures and their electrochemical performance, J. Electroanal. Chem. 771 (2016) 106–113.
[32] Y. Wang, M. Zhang, X. Shen, H. Wang, H. Wang, K. Xia, Z. Yin, Y. Zhang, Biomass-derived carbon materials: controllable preparation and versatile applications, Small. 17 (2021) 1–32.
[33] A.M. Smith, S. Singh, A.B. Ross, Fate of inorganic material during hydrothermal carbonisation of biomass: influence of feedstock on combustion behaviour of hydrochar, Fuel. 169 (2016) 135–145.
[34] R. Sharma, K. Jasrotia, N. Singh, P. Ghosh, S. Srivastava, N.R. Sharma, J. Singh, R. Kanwar, A. Kumar, A Comprehensive Review on Hydrothermal Carbonization of Biomass and its Applications, Chem. Africa. 3 (2020).
[35] X. Sun, Y. Li, Colloidal carbon spheres and their Core/Shell structures with Noble-metal nanoparticles, Angew. Chem. Int. Ed. 43 (2004) 597–601.
[36] H. Guan, Q. Wang, X. Wu, J. Pang, Z. Jiang, G. Chen, C. Dong, L. Wang, C. Gong, Biomass derived porous carbon (BPC) and their composites as lightweight and efficient microwave absorption materials, Compos. Part B Eng. 207 (2021) 108562.
[37] J.H. Knox, B. Kaur, G.R. Millward, Structure and performance of porous graphitic carbon in liquid chromatography, J. Chromatogr. A 352 (1986) 3–25.

[38] Z.E. Tang, S. Lim, Y.L. Pang, H.C. Ong, K.T. Lee, Synthesis of biomass as heterogeneous catalyst for application in biodiesel production: state of the art and fundamental review, Renew. Sust. Energ. Rev. 92 (2018) 235–253.
[39] S. Feng, W. Li, J. Wang, Y. Song, A.A. Elzatahry, Y. Xia, D. Zhao, Hydrothermal synthesis of ordered mesoporous carbons from a biomass-derived precursor for electrochemical capacitors, Nanoscale. 6 (2014) 14657–14661.
[40] L. Du, G. Zhang, X. Liu, A. Hassanpour, M. Dubois, A.C. Tavares, S. Sun, Biomass-derived nonprecious metal catalysts for oxygen reduction reaction: the demand-oriented engineering of active sites and structures, Carbon Energy. 2 (2020) 561–581.
[41] X. Zhao, W. Li, F. Kong, H. Chen, Z. Wang, S. Liu, C. Jin, Carbon spheres derived from biomass residue via ultrasonic spray pyrolysis for supercapacitors, Mater. Chem. Phys. 219 (2018) 461–467.
[42] R. Wang, W. Li, S. Liu, A porous carbon foam prepared from liquefied birch sawdust, J. Mater. Sci. 47 (2012) 1977–1984.
[43] X. Tang, D. Liu, Y.J. Wang, L. Cui, A. Ignaszak, Y. Yu, J. Zhang, Research advances in biomass-derived nanostructured carbons and their composite materials for electrochemical energy technologies, Prog. Mater. Sci. 118 (2021) 100770.
[44] J. Li, R. Xiao, M. Li, H. Zhang, S. Wu, C. Xia, Template-synthesized hierarchical porous carbons from bio-oil with high performance for supercapacitor electrodes, Fuel Process. Technol. 192 (2019) 239–249.
[45] M. Chen, D. Yu, X. Zheng, X. Dong, Biomass based N-doped hierarchical porous carbon nanosheets for all-solid-state supercapacitors, J. Energy Storag. 21 (2019) 105–112.
[46] J. Luo, H. Zhang, Z. Zhang, J. Yu, Z. Yang, In-built template synthesis of hierarchical porous carbon microcubes from biomass toward electrochemical energy storage, Carbon. 155 (2019) 1–8.
[47] Y. Qu, M. Guo, X. Wang, C. Yuan, Novel nitrogen-doped ordered mesoporous carbon as high-performance anode material for sodium-ion batteries, J. Alloys Compd. 791 (2019) 874–882.
[48] X. Bai, Z. Wang, J. Luo, W. Wu, Y. Liang, X. Tong, Z. Zhao, Hierarchical porous carbon with interconnected ordered pores from biowaste for high-performance supercapacitor electrodes, Nanoscale Res. Lett. 15 (2020).
[49] J. Lee, K.H. Kim, E.E. Kwon, Biochar as a catalyst, Renew. Sust. Energ. Rev. 77 (2017) 70–79.
[50] W.J. Liu, H. Jiang, H.Q. Yu, Development of biochar-based functional materials: toward a sustainable platform carbon material, Chem. Rev. 115 (2015) 12251–12285.
[51] S. Rezma, M. Birot, A. Hafiane, H. Deleuze, Physically activated microporous carbon from a new biomass source: date palm petioles, C. R. Chim. 20 (2017) 881–887.
[52] N.T. Mai, M.N. Nguyen, T. Tsubota, P.L.T. Nguyen, N.H. Nguyen, Evolution of physico-chemical properties of Dicranopteris linearis-derived activated carbon under various physical activation atmospheres, Sci. Rep. 11 (2021) 1–9.
[53] X. Cao, S. Sun, R. Sun, Application of biochar-based catalysts in biomass upgrading: a review, RSC Adv. 7 (2017) 48793–48805.
[54] J.S. Cha, S.H. Park, S.-C. Jung, C. Ryu, J.-K. Jeon, M.-C. Shin, Y.-K. Park, Production and utilization of biochar: a review, J. Ind. Eng. Chem. 40 (2016) 1–15.
[55] A.M. Dehkhoda, N. Ellis, E. Gyenge, Electrosorption on activated biochar: effect of thermo-chemical activation treatment on the electric double layer capacitance, J. Appl. Electrochem. 44 (2014) 141–157.
[56] J.H. Park, Y.S. Ok, S.H. Kim, J.S. Cho, J.S. Heo, R.D. Delaune, D.C. Seo, Evaluation of phosphorus adsorption capacity of sesame straw biochar on aqueous solution: influence of activation methods and pyrolysis temperatures, Environ. Geochem. Health 37 (2015) 969–983.
[57] Y. Sun, H. Li, G. Li, B. Gao, Q. Yue, X. Li, Characterization and ciprofloxacin adsorption properties of activated carbons prepared from biomass wastes by H3PO4 activation, Bioresour. Technol. 217 (2016) 239–244.
[58] M. Mittal, S. Sardar, A. Jana, Chapter 7 - nanofabrication techniques for semiconductor chemical sensors, in: C.M. Hussain, S.K.B.T.-H. of N. for S.A. Kailasa (Eds.), Micro and Nano Technologies, Elsevier, 2021, pp. 119–137.
[59] H. Nishihara, T. Kyotani, Zeolite-templated carbons – three-dimensional microporous graphene frameworks, Chem. Commun. 54 (2018) 5648–5673.
[60] T. Aumond, J. Rousseau, Y. Pouilloux, L. Pinard, A. Sachse, Synthesis of hierarchical zeolite templated carbons, Carbon Trends. 2 (2021) 100014.
[61] P.X. Hou, T. Yamazaki, H. Orikasa, T. Kyotani, An easy method for the synthesis of ordered microporous carbons by the template technique, Carbon. 43 (2005) 2624–2627.
[62] Z. Chen, W. Wei, B.-J. Ni, H. Chen, Plastic wastes derived carbon materials for green energy and sustainable environmental applications, Environ. Funct. Mater. 1 (2022) 34–48.
[63] R. Acosta, D. Nabarlatz, A. Sánchez-Sánchez, J. Jagiello, P. Gadonneix, A. Celzard, V. Fierro, Adsorption of bisphenol a on KOH-activated Tyre pyrolysis char, journal of environmental, Chem. Eng. 6 (2018) 823–833.
[64] G. Li, S. Tan, R. Song, T. Tang, Synergetic effects of molybdenum and magnesium in Ni–Mo–mg catalysts on the one-step carbonization of polystyrene into carbon nanotubes, Ind. Eng. Chem. Res. 56 (2017) 11734–11744.
[65] R. Yu, X. Wen, J. Liu, Y. Wang, X. Chen, K. Wenelska, E. Mijowska, T. Tang, A green and high-yield route to recycle waste masks into CNTs/Ni hybrids via catalytic carbonization and their application for superior microwave absorption, Appl. Catal. B Environ. 298 (2021) 120544.
[66] C. Jia, K. Dastafkan, W. Ren, W. Yang, C. Zhao, Carbon-based catalysts for electrochemical CO2 reduction, Sustain. Energ. Fuel 3 (2019) 2890–2906.
[67] L. Luo, Y. Lan, Q. Zhang, J. Deng, L. Luo, Q. Zeng, H. Gao, W. Zhao, A review on biomass-derived activated carbon as electrode materials for energy storage supercapacitors, J. Energy Storag. 55 (2022).
[68] D.R. Lobato-Peralta, E. Duque-Brito, H.O. Orugba, D.M. Arias, A.K. Cuentas-Gallegos, J.A. Okolie, P.U. Okoye, Sponge-like nanoporous activated carbon from corn husk as a sustainable and highly stable supercapacitor electrode for energy storage, Diam. Relat. Mater. 138 (2023).
[69] C. Zhan, X. Yu, Q. Liang, W. Liu, Y. Wang, R. Lv, Z.H. Huang, F. Kang, Flour food waste derived activated carbon for high-performance supercapacitors, RSC Adv. 6 (2016) 89391–89396.
[70] G. Li, Y. Li, X. Chen, X. Hou, H. Lin, L. Jia, One step synthesis of N, P co-doped hierarchical porous carbon nanosheets derived from pomelo peel for high performance supercapacitors, J. Colloid Interface Sci. 605 (2022) 71–81.
[71] S.S. Desa, T. Ishii, K. Nueangnoraj, Sulfur-doped carbons from durian peels, their surface characteristics, and electrochemical behaviors, ACS Omega. 6 (2021) 24902–24909.
[72] Y.-M. Zhao, T.-Z. Ren, Z.-Y. Yuan, T.J. Bandosz, Activated carbon with heteroatoms from organic salt for hydrogen evolution reaction, Microporous Mesoporous Mater. 297 (2020) 110033.
[73] Y. Zhou, Y. Leng, W. Zhou, J. Huang, M. Zhao, J. Zhan, C. Feng, Z. Tang, S. Chen, H. Liu, Sulfur and nitrogen self-doped carbon nanosheets derived from peanut root nodules as high-efficiency non-metal electrocatalyst for hydrogen evolution reaction, Nano Energy 16 (2015) 357–366.
[74] X. Chen, B. Yu, Y. Dong, X. Zhu, W. Zhang, S. Ramakrishna, Z. Liu, Electrospun porous carbon nanofibers decorated with iron-doped cobalt phosphide nanoparticles for hydrogen evolution, J. Alloys Compd. 918 (2022) 165733.
[75] T. Wang, Z. Chen, W. Gong, F. Xu, X. Song, X. He, M. Fan, Electrospun carbon nanofibers and their applications in several areas, ACS Omega 8 (2023) 22316–22330.
[76] M. Gao, C.K.N. Peh, W.L. Ong, G.W. Ho, Green chemistry synthesis of a nanocomposite graphene hydrogel with three-dimensional nano-mesopores for photocatalytic H2 production, RSC Adv. 3 (2013) 13169–13177.
[77] P. Kuang, M. Sayed, J. Fan, B. Cheng, J. Yu, 3D graphene-based H2-production Photocatalyst and Electrocatalyst, Adv. Energy Mater. 10 (2020) 1903802.
[78] S.F. Ahmed, P.S. Kumar, B. Ahmed, T. Mehnaz, G.M. Shafiullah, V.N. Nguyen, X. Q. Duong, M. Mofijur, I.A. Badruddin, S. Kamangar, Carbon-based nanomaterials: characteristics, dimensions, advances and challenges in enhancing photocatalytic hydrogen production, Int. J. Hydrog. Energy 52 (2024) 424–442.
[79] C.-J. Chang, Y.-G. Lin, H.-T. Weng, Y.-H. Wei, Photocatalytic hydrogen production from glycerol solution at room temperature by ZnO-ZnS/graphene photocatalysts, Appl. Surf. Sci. 451 (2018) 198–206.
[80] S. Pandey, M. Karakoti, S. Dhali, N. Karki, B. SanthiBhushan, C. Tewari, S. Rana, A. Srivastava, A.B. Melkani, N.G. Sahoo, Bulk synthesis of graphene nanosheets from plastic waste: an invincible method of solid waste management for better tomorrow, Waste Manag. 88 (2019) 48–55.
[81] O.A. Nerushev, S. Dittmar, R.E. Morjan, F. Rohmund, E.E.B. Campbell, Particle size dependence and model for iron-catalyzed growth of carbon nanotubes by thermal chemical vapor deposition, J. Appl. Phys. 93 (2003) 4185–4190.
[82] J. Liu, Z. Jiang, H. Yu, T. Tang, Catalytic pyrolysis of polypropylene to synthesize carbon nanotubes and hydrogen through a two-stage process, Polym. Degrad. Stab. 96 (2011) 1711–1719.
[83] Y. Zhang, C. Wu, M.A. Nahil, P. Williams, Pyrolysis–Catalytic Reforming/Gasification of Waste Tires for Production of Carbon Nanotubes and Hydrogen, Energy Fuel 29 (2015) 3328–3334.
[84] D.A.C. Brownson, S.A. Varey, F. Hussain, S.J. Haigh, C.E. Banks, Electrochemical properties of CVD grown pristine graphene: monolayer- vs. quasi-graphene, Nanoscale. 6 (2014) 1607–1621.
[85] A. Islam, S.H. Teo, Y.H. Taufiq-Yap, C.H. Ng, D.V.N. Vo, M.L. Ibrahim, M. M. Hasan, M.A.R. Khan, A.S.M. Nur, M.R. Awual, Step towards the sustainable toxic dyes and heavy metals removal and recycling from aqueous solution- a comprehensive review, Resour. Conserv. Recycl. 175 (2021) 105849.
[86] B. Wang, J. Lan, C. Bo, B. Gong, J. Ou, Adsorption of heavy metal onto biomass-derived activated carbon, RSC Adv. 13 (2023) 4275–4302.
[87] A. Gómez-Avilés, M. Peñas-Garzón, C. Belver, J.J. Rodriguez, J. Bedia, Equilibrium, kinetics and breakthrough curves of acetaminophen adsorption onto activated carbons from microwave-assisted FeCl3-activation of lignin, Sep. Purif. Technol. 278 (2021) 119654.
[88] N.U.M. Nizam, M.M. Hanafiah, E. Mahmoudi, A.A. Halim, A.W. Mohammad, The removal of anionic and cationic dyes from an aqueous solution using biomass-based activated carbon, Sci. Rep. 11 (2021) 1–17.
[89] Z. Cai, X. Deng, Q. Wang, J. Lai, H. Xie, Y. Chen, B. Huang, G. Lin, Core-shell granular activated carbon and its adsorption of trypan blue, J. Clean. Prod. 242 (2020).
[90] S.H. Teo, C.H. Ng, A. Islam, G. Abdulkareem-Alsultan, C.G. Joseph, J. Janaun, Y. H. Taufiq-Yap, S. Khandaker, G.J. Islam, H. Znad, M.R. Awual, Sustainable toxic dyes removal with advanced materials for clean water production: a comprehensive review, J. Clean. Prod. 332 (2022).
[91] C. Xu, C. Jiao, R. Yao, A. Lin, W. Jiao, Adsorption and regeneration of expanded graphite modified by CTAB-KBr/H3PO4 for marine oil pollution, Environ. Pollut. 233 (2018) 194–200.
[92] L.-C. Wang, X. Ni, Y.-H. Cao, G. Cao, Adsorption behavior of bisphenol a on CTAB-modified graphite, Appl. Surf. Sci. 428 (2018) 165–170.
[93] A.V. Ivanov, S.I. Volkova, N.V. Maksimova, K.V. Pokholok, A.V. Kravtsov, A. A. Belik, S.M. Posokhova, I.L. Kalachev, V.V. Avdeev, Exfoliated graphite with γ-Fe_2O_3 for the removal of oil and organic pollutants from the water surface:

synthesis, Mossbauer study, sorption and magnetic properties, J. Alloys Compd. 960 (2023) 170619.
[94] F. Liu, Z. Guo, H. Ling, Z. Huang, D. Tang, Effect of pore structure on the adsorption of aqueous dyes to ordered mesoporous carbons, Microporous Mesoporous Mater. 227 (2016) 104–111.
[95] D. Luo, X. Zhang, The effect of oxygen–containing functional groups on the H2 adsorption of graphene–based nanomaterials: experiment and theory, Int. J. Hydrog. Energy 43 (2018) 5668–5679.
[96] S. Wang, X. Li, Y. Liu, C. Zhang, X. Tan, G. Zeng, B. Song, L. Jiang, Nitrogen-containing amino compounds functionalized graphene oxide: synthesis, characterization and application for the removal of pollutants from wastewater: a review, J. Hazard. Mater. 342 (2018) 177–191.
[97] K. Molaei, H. Bagheri, A.A. Asgharinezhad, H. Ebrahimzadeh, M. Shamsipur, SiO2-coated magnetic graphene oxide modified with polypyrrole–polythiophene: a novel and efficient nanocomposite for solid phase extraction of trace amounts of heavy metals, Talanta. 167 (2017) 607–616.
[98] X. Liu, R. Ma, X. Wang, Y. Ma, Y. Yang, L. Zhuang, S. Zhang, R. Jehan, J. Chen, X. Wang, Graphene oxide-based materials for efficient removal of heavy metal ions from aqueous solution: a review, Environ. Pollut. 252 (2019) 62–73.
[99] A.I.A. Sherlala, A.A.A. Raman, M.M. Bello, A. Asghar, A review of the applications of organo-functionalized magnetic graphene oxide nanocomposites for heavy metal adsorption, Chemosphere. 193 (2018) 1004–1017.
[100] C. Zhou, H. Zhu, Q. Wang, J. Wang, J. Cheng, Y. Guo, X. Zhou, R. Bai, Adsorption of mercury(ii) with an Fe3O4 magnetic polypyrrole–graphene oxide nanocomposite, RSC Adv. 7 (2017) 18466–18479.
[101] M.D. Faysal Hossain, N. Akther, Y. Zhou, Recent advancements in graphene adsorbents for wastewater treatment: current status and challenges, Chin. Chem. Lett. 31 (2020) 2525–2538.
[102] J. Yao, Y. Chen, H. Yu, T. Liu, L. Yan, B. Du, Y. Cui, Efficient and fast removal of Pb(ii) by facile prepared magnetic vermiculite from aqueous solution, RSC Adv. 6 (2016) 101353–101360.
[103] S. Wei, A.R. Kamali, Waste plastic derived Co3Fe7/CoFe2O4@carbon magnetic nanostructures for efficient dye adsorption, J. Alloys Compd. 886 (2021) 161201.
[104] A. Rezaei, B. Kamali, A.R. Kamali, Correlation between morphological, structural and electrical properties of graphite and exfoliated graphene nanostructures, Measurement. 150 (2020) 107087.
[105] J. Kang, L. Zhou, X. Duan, H. Sun, Z. Ao, S. Wang, Degradation of cosmetic microplastics via functionalized carbon Nanosprings, Matter. 1 (2019) 745–758.
[106] A.G. Adeniyi, K.O. Iwuozor, E.C. Emenike, O.J. Ajala, S. Ogunniyi, K.B. Muritala, Thermochemical co-conversion of biomass-plastic waste to biochar: a review, Green Chem. Eng. (2023).